environments

Article

Spatiotemporal Distribution and Ecological Risks of Trace Metals in a Marine Protected Area of the Northwestern Arabian Gulf

Turki Al-Said [1], Surendraraj Alagarsamy [1,*], Sabeena Farvin Koduvayur Habeebullah [1], Ali Al-Hashem [1], Loreta Fernandes [1], Amit Sarkar [1], Yesudhason Poulose [2], Rakhesh Madhusoodanan [1], Waleed Al-Zakri [1] and Faiza Al-Yamani [1]

[1] Coastal and Marine Resource Program, Environment and Life Sciences Research Center, Kuwait Institute for Scientific Research, P.O. Box 1638, Salmiya 22017, Kuwait; trsaid@kisr.edu.kw (T.A.-S.); shabeebullah@kisr.edu.kw (S.F.K.H.); alhashem@kisr.edu.kw (A.A.-H.); lfernandes@kisr.edu.kw (L.F.); amitsarkar81@gmail.com (A.S.); rmdhanan@kisr.edu.kw (R.M.); wzakri@kisr.edu.kw (W.A.-Z.); faizayamani@gmail.com (F.A.-Y.)
[2] Quality, Health, Safety and Work Environment Department, Science and Technology Sector, Kuwait Institute for Scientific Research, P.O. Box 1638, Salmiya 22017, Kuwait; ypoulose@kisr.edu.kw
* Correspondence: salagarsamy@kisr.edu.kw

Abstract

Dissolved bio-essential trace metals (Cu, Zn, Co, Ni, and Fe) in seawater and 17 elements in surface sediments were studied to assess the metal contamination and associated ecological risks in the Sulaibikhat Bay Marine Protected Area (MPA) in the northwestern Arabian Gulf. Dissolved metals were mostly at low to moderate levels and within the limits of most international water quality standards. However, dissolved Cu concentrations (0.54 to 4.73 μg L^{-1}) in the MPA stations (MPA-1 and MPA-2) exceeded the Oslo–Paris Convention for the Protection of the Marine Environment of the North-East Atlantic (OSPAR) ecotoxicological assessment thresholds, suggesting possible adverse ecological effects. Sediment showed higher levels of Cd, Cr, Ni, V, Cu, and Zn at stations within the MPA, with Principal Component Analysis (PCA) linking these enrichments to nearby industrial and desalination discharge sources. The calculated enrichment factor (EF) and geoaccumulation index (I_{geo}) values confirmed moderate to substantial anthropogenic contributions for Cd, Cr, and Ni, while the major lithogenic elements were derived from natural mineralogical inputs. A pollution load index (PLI) > 1 at stations MPA-1, MPA-3 and MPA-4 in Sulaibikhat Bay indicated cumulative metal contamination. Ecological risk assessment criteria classified sediments within the MPA and Sulaibikhat Bay as having a moderate level of ecological risk, with Cd identified as the principal contributor. The toxicological indices, namely mean Effect Range Median Quotient (m-ERM-Q) and mean Probable Effect Level Quotient (m-PEL-Q), indicated a low-to-moderate probability of adverse biological effects due to Cu and Ni exposure in the MPA. In contrast, the reference station in the Kuwait Bay showed very low contamination and negligible ecological risk. These findings stress the need for continuous monitoring and effective source control to protect the ecosystem of this newly established MPA in Kuwait.

Keywords: marine protected area; metal contamination; sediment quality indices; ecological risk assessment; anthropogenic impact

Check for updates

Academic Editor: Claude Fortin

Received: 16 May 2026
Revised: 21 June 2026
Accepted: 22 June 2026
Published: 22 July 2026

Copyright: © 2026 by the authors. Licensee MDPI, Basel, Switzerland. This article is an open access article distributed under the terms and conditions of the Creative Commons Attribution (CC BY) license.

1. Introduction

Marine ecosystems are among the most productive and biologically diverse habitats on Earth, and deliver vital services that sustain both marine life and human populations. However, increasing anthropogenic pressures, particularly pollution, are degrading these systems and threatening the sustainability of their resources [1]. To address these challenges, Marine Protected Areas (MPAs) have been widely adopted as an effective strategy for conserving biodiversity and maintaining ecosystem services [2]. When effectively planned and managed, MPAs support fisheries, maintain ecological balance, and provide direct benefits to coastal communities [2,3]. Yet, MPA effectiveness varies regionally and is influenced by environmental conditions (water quality and sediment characteristics) and the strength of management through national regulations and regional cooperation [3–6].

Contaminants entering MPAs or surrounding areas pose significant threats to marine ecosystems, as their toxic effects can compromise ecological integrity [5,7–9]. Among chemical contaminants, metals pose substantial risks to marine organisms due to accumulation in sediments and the water column [7,8]. Global studies have documented elevated concentrations of trace metals in coastal sediments, including those within MPAs, raising concerns about their ability to meet conservation objectives [4,5,8,10]. Elevated levels of copper (Cu), lead (Pb), and zinc (Zn) have been documented within an MPA in Australia with boating infrastructure, resulting in shifts in benthic infaunal assemblages even after spatial management/zoning [11]. Similar metal contamination events have been reported in MPAs in the Bay of Bengal, Bangladesh; the East Indian Archipelago, Indonesia; the Bohai Sea, China; and the Ross Sea, Antarctica, indicating that MPAs are not exempt from pollution pressures [4,10,12,13]. In southeastern Brazil, concentrations of cadmium (Cd), chromium (Cr), Cu, Pb, and Zn were higher within MPAs [8], while sediments in the coastal waters of the western Arabian Gulf [14] and the central Arabian Gulf [15] showed elevated levels of aluminium (Al), iron (Fe), manganese (Mn), and arsenic (As). Metals including Cd, Pb, mercury (Hg), Cu, Zn, and nickel (Ni) remain major environmental concerns because they resist degradation, build up in aquatic systems, and can harm organisms from benthic fauna to humans [11,16–18].

The Arabian Gulf is the world's hottest sea during summer [19] and is recognised as one of the most environmentally stressed and vulnerable marine regions [15,20]. The Sulaibikhat MPA, the first MPA established in Kuwait in the northwestern Arabian Gulf, is exposed to intense natural and human-induced stressors, including extreme salinity, high temperatures, land reclamation, urban expansion, desalination activities, and pollution from multiple sources [20–23]. Elevated Hg levels associated with historical inputs from desalination plants and other industrial discharges have been reported in marine sediments [24]. A recent study by Habeebullah et al. [25] highlighted ongoing contamination in the Sulaibikhat MPA, reporting high concentrations of petroleum hydrocarbons, polycyclic aromatic hydrocarbons, polychlorinated biphenyls, pesticides, and other persistent organic pollutants at concentrations exceeding safety thresholds, and stressed the need for long-term management to mitigate the pollution threats for protecting the ecosystems and human health. Though several studies have investigated metal contamination in Sulaibikhat Bay, the Sulaibikhat MPA has received limited scientific attention. As the newly established MPA is located in a semi-enclosed embayment characterised by fine-grained sediments, limited tidal flushing, and proximity to multiple pollution sources [26], we hypothesised that trace metal concentrations and associated ecological risks would vary spatially and seasonally because of differences in anthropogenic inputs and hydrodynamic conditions. This study provides the first comprehensive assessment of trace metals in the water and sediment of the Sulaibikhat Bay MPA, along with an ecological risk evaluation. These are essential for establishing a critical baseline for future monitoring and for develop-

ing effective management strategies to enhance ecosystem resilience in the northwestern Arabian Gulf.

2. Materials and Methods

2.1. The Study Area

A 280 ha section of Sulaibikhat Bay was recently designated as an MPA. It is rectangular in shape (NW: 29.35278° N, 47.82250° E; SW: 29.34361° N, 47.82250° E; NE: 29.35278° N, 47.84258° E; and SE: 29.34361° N, 47.84528° E) and is a biologically rich intertidal mudflat in Kuwait (Figure 1).

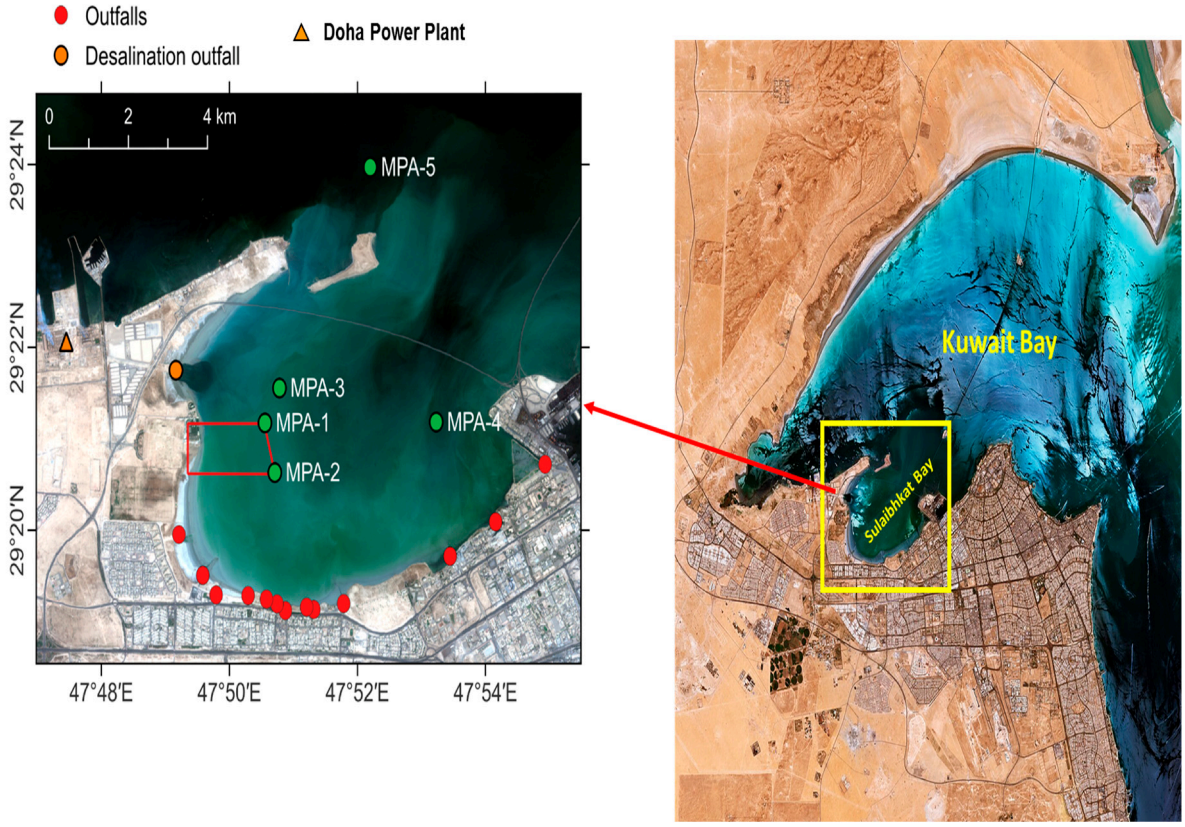


Figure 1. Sampling stations located in and around the Marine Protected Area (MPA) of Sulaibikhat Bay. The red rectangle indicates the boundary of the Sulaibikaht Bay MPA.

It is shallow with water depths generally less than 3 m, and experiences minimal wave activity due to the natural sheltering effect of the bay. Hydrodynamics are primarily governed by tidal currents, with additional density-driven circulation resulting from the release of concentrated brine from the adjacent desalination facility. In the present study, five sampling stations, designated as MPA-1 to MPA-5, were established in and around the MPA (Figure 1). Stations MPA-1 and MPA-2 are located within the MPA boundaries. MPA-3 is positioned near the outfall of the Doha power and Desalination plant, while MPA-4 is located in the eastern part of the bay near the Al-Ghazali sewage outfall. These two stations are inside the Sulaibikhat Bay. MPA-5, located outside the bay, serves as a reference site for comparison with Kuwait Bay.

Sampling stations MPA-1 to MPA-4 were characterised by clayey substrates, whereas MPA-5 had a sandy bottom. The surface water temperature, pH, and salinity in the study area ranged from 18 to 32 °C, 7.54 to 8.77, and 42 to 45 ppt, respectively [27].

2.2. Sample Collection and Processing

Five stations in and around were sampled between October 2018 and March 2021. Seawater samples for metals were collected monthly, while sediment samples were collected quarterly. All the analyses were carried out in duplicate. Seawater for dissolved metal analysis was collected using an acid-cleaned polythene sampler. From this, 500 mL seawater was transferred to an acid-cleaned, low-density polythene bottle (LDPE, Nalgene, Thermo Fisher Scientific, Rochester, NY, USA) and was filtered through acid-cleaned 0.4-µm polycarbonate filters (Whatman, Maidstone, UK). The filtrate was divided into two. 250 mL was preserved with 6N HCl (Romil Ltd., Cambridge, UK) for the analysis of dissolved trace metals (Cu, Ni, Co, and Zn) by Ad-CSV. The other half is preserved with concentrated HCl (12N HCl) for the analysis of iron by a flow injection analyser. All trace metal sample handling and preparation procedures were performed in a laminar-flow hood to minimise contamination. All samples were adjusted to a pH below 2 and stored at room temperature (20–23 °C) until analysis [21].

Sediment cores were collected using a handheld gravity coring system (USC06000; UWITEC GmbH, Mondsee, Austria). Immediately upon retrieval, the upper 2 cm of each core was sectioned and transferred to a pre-cleaned plastic container. The samples were subsequently frozen, freeze-dried, and preserved until analysis. Analysis was carried out in duplicate. Sediment core collection at MPA-5 was technically challenging because of the sandy substrate. Sediment cores were successfully retrieved in winter, summer, and fall after multiple attempts; however, spring sampling was unsuccessful.

2.3. Analysis of Dissolved Trace Metals in Seawater and Quality Control

A custom-built UV digestion unit that accommodates eight samples per cycle was used for sample digestion. Quartz tubes (approximately 30 mL in capacity), arranged around the UV lamp, were filled with the sample and exposed to ultraviolet radiation for 4–5 h. The digested seawater samples were analysed for dissolved trace metals by adsorptive cathodic stripping voltammetry (Ad-CSV) [21]. Quantification of Co, Cu, Ni, and Zn was performed using the standard addition method. A metal standard of known concentration was added to the voltammetric cell, and the increase in peak response was recorded. The linearity of the analytical response was verified by a second standard addition within the same cell. Metal concentrations of the samples were then calculated by extrapolation [21].

Total dissolved Fe concentrations were analysed using an automated flow injection analyser (FIA) equipped with luminol-based chemiluminescence detection (Waterville Analytical, Waterville, ME, USA). Prior to analysis, samples were pre-concentrated on a Toyopearl AF 650-M resin column (Tosoh Bioscience, Tokyo, Japan) to enhance analytical sensitivity. This method detects the chemiluminescence generated when iron reacts with luminol in the presence of hydrogen peroxide. The emitted light intensity is proportional to the iron concentration and was quantified using the standard addition method [21]. A seawater-certified reference material, CASS-6 (National Research Council Canada, Ottawa, ON, Canada), was used alongside the samples, and percentage recoveries were calculated to assess method performance (Table S1).

2.4. Analysis of Sedimentary Metals and Quality Control

Sedimentary trace metals strontium (Sr), molybdenum (Mo), Cd, barium (Ba), Pb, thorium (Th), uranium (U), Al, vanadium (V), Mn, titanium (Ti), chromium (Cr), Fe, cobalt (Co), Ni, Cu, and Zn were analyzed following the protocol recommended by the GEOTRACES program (2017) [28]. Freeze–dried sediments were ground into a fine powder and digested using a microwave-assisted acid digestion procedure prior to metal analysis [29]. Aliquots of sediment (10–30 mg) were weighed directly into the digestion vials. Each sample was

treated with 5 mL of an acid mixture containing 4 M nitric acid, 4 M hydrochloric acid, and 4 M hydrofluoric acid, and digested at 180 °C for 4 h. Following digestion, the samples were evaporated to near dryness. Subsequently, 1 mL of an oxidising mixture (50% HNO_3 and 15% H_2O_2, *v*/*v*) was added to each sample, which was again evaporated to dryness. The residues were redissolved and diluted to a final volume of 9 mL before analysis by high-resolution inductively coupled plasma mass spectrometry (HR-ICP-MS; Element XR, Thermo Fisher Scientific, Bremen, Germany) at GEOMAR, Germany. Analytical accuracy and precision were verified using the certified reference material PACS-3 (National Research Council Canada, Ottawa, ON, Canada). The measured elemental concentrations showed good agreement with the certified reference values, confirming the reliability of the analytical procedures (Table S2).

Principal component analysis (PCA) was performed on sediment metal composition data from different sampling stations using Unscrambler X (AspenTech, Bedford, MA, USA). Full cross-validation was applied, and the variables were standardised by dividing each variable by its standard deviation.

2.5. Determination of Environmental Contamination Indices

The degree of metal enrichment and the associated ecological risks were assessed using several environmental contamination indices, including the enrichment factor (EF), geoaccumulation index (I_{geo}), pollution load index (PLI), and ecological risk index (RI). These indices were calculated using the following equations.

2.5.1. Enrichment Factor (EF)

The EF is a widely used index in environmental geochemistry to assess the degree of metal contamination in sediments, soils, dust, and, occasionally, in water. It helps determine whether the concentration of a metal in a sample originates from natural (geogenic) sources or anthropogenic (human-induced) activities [30].

$$\mathrm{EF} = (C_m / C_{ref})_{\text{ Sample}}$$

$$(C_m / C_{ref})_{\text{ Background}}$$

where C_m is the concentration of the target metal, C_{ref} is the concentration of the reference metal.

In this study, iron (Fe) was used as the reference element for geochemical normalisation. There are several reasons for selecting Fe as a reference metal. It is among the most abundant elements in the Earth's crust and is associated with clay minerals. Iron's geochemical behaviour is comparable to that of other trace metals, and natural Fe concentrations tend to be relatively stable, providing a reliable baseline for comparison. The average elemental concentrations of the upper continental crust (UCC) reported by Rudnick and Gao [31] were used as the background concentrations. UCC values were used as background values in this study because site-specific pre-industrial baseline data are unavailable for the study area.

2.5.2. Geoaccumulation Index (I_{geo})

I_{geo} is widely used to evaluate the degree of metal contamination in soils and sediments [30]. This index was calculated using the following formula:

$$I_{geo} = \log_2 (C_n / 1.5B_n)$$

where C_n represent the measured concentration of the element (mg/kg or ug/g), B_n denotes the corresponding background concentration, 1.5 is a correction factor that accounts for natural variability in the background values.

The average UCC element values reported by Rudnick and Gao [31] were used as background concentrations.

2.5.3. Pollution Load Index (PLI)

PLI was applied to evaluate the overall level of metal contamination in each sampling site. It was derived from the contamination factors (CFs) of individual metals at each sampling site as described by Elobaid et al. [15]. CF and PLI were calculated as follows:

$$\text{Contamination factor of each metal } (CF_i) = C_i / B_i$$

where C_i is the measured concentration of metal "i" in the sample. B_i is the background concentration of metal i. The average UCC element values reported by Rudnick and Gao [31] were used as background concentrations.

The PLI is the geometric mean of the CF values for n elements and is calculated using the following equation.

$$PLI = (CF_1 \times CF_2 \times CF_3 \times \ldots \times CF_n)^{1/n}$$

where CF is the contamination factor of each element. n is the total number of elements studied (n = 16 in this study).

2.5.4. Potential Ecological Risk Index

To understand the ecological risk posed by multiple trace metals in the sediments, the ecological risk index (RI) was estimated using the following equation [32]:

$$RI = \sum_i^n Er^i = \sum_i^n Tr^i * CF^i$$

where Er is the potential ecological risk factor of a given element. Tr is the toxic response factor for a given metal, and CF is the contamination factor. The Tr values for Cd, Ni, Pb, Cr, and Zn were set to 30, 5, 5, 2, and 1, respectively [32,33].

2.6. Determination of Toxicological Risk Indices

Potential ecological risks associated with metal contamination in sediments were evaluated using sediment quality guidelines (SQGs). Specifically, the threshold effect level (TEL), probable effect level (PEL), effect range low (ERL), and effect range median (ERM), were applied [34]. In this study, SQGs were obtained from SQuiRTs values for inorganic contaminants in marine sediments [35] (Table 1). These guideline values serve as reference standards for assessing the adverse effects on aquatic organisms within an ecosystem.

Table 1. The sediment quality guidelines (SQGs) assessment criteria for metals.

Metal	TEL (mg kg^{-1})	PEL (mg kg^{-1})	ERL (mg kg^{-1})	ERM (mg kg^{-1})
Cd	0.7	4.2	1.2	9.6
Pb	30.2	112.0	46.7	218.0
Cr	52.3	160.0	81.0	370.0
Ni	15.9	42.8	20.9	51.6
Cu	18.7	108.0	34.0	270.0
Zn	124.0	271.0	150.0	410.0

Where ERL (Effects Range Low): Concentration below which adverse biological effects are rarely observed. ERM (Effects Range Median): Concentration above which biological effects are expected to occur frequently. PEL (Probable Effect Level): Concentration of a contaminant in sediment above which adverse biological effects are likely to occur frequently in benthic organisms. TEL (Threshold Effect Level): Concentration of a contaminant in sediment below which adverse biological effects are expected to occur rarely in aquatic organisms.

The measured metal concentrations were compared with their corresponding ERL and ERM values to identify metals that may pose potential ecological risks in the study area. The overall toxicological risk associated with multiple metals was further evaluated using the mean ERM quotient (m-ERM-Q) and the mean PEL quotient (m-PEL-Q) indices [15]:

$$m - ERM - Q = 1/n \sum_{i}^{n} Ci/ERMi$$

$$m - PEL - Q = 1/n \sum_{i}^{n} Ci/PELi$$

where Ci is the concentration of element "i" in the sample, and n is the total number of elements.

3. Results and Discussion

3.1. Dissolved Trace Metals in Seawater

Trace metals, such as Cu, Fe, Co, Ni, and Zn, are bioessential micronutrients that play important roles in regulating marine productivity and biogeochemical cycling. Although present at low concentrations, these metals play vital roles in photosynthesis, respiration, nitrogen metabolism, and enzymatic reactions by serving as cofactors for numerous enzymes [36]. Their bioavailability controls phytoplankton and macroalgal growth and community composition, ultimately influencing trophic structure and carbon sequestration in marine systems [21]. Different natural and anthropogenic factors determine the distribution of trace metals in seawater. Natural sources include river discharge, atmospheric dust deposition, and sediment water interactions, whereas anthropogenic sources include industrial effluents, urban runoff, maritime activities, and oil-related contamination [37,38]. Therefore, monitoring Cu, Fe, Co, Ni, and Zn concentrations provides valuable information on seawater quality, ecosystem health, and potential pollution impacts in coastal environments. To evaluate the status of these bioessential trace metals in the Sulaibikhat Bay MPA, dissolved concentrations of Cu, Zn, Co, Ni, and Fe were measured over a 26-month period (October 2018–March 2021).

The metal concentrations and their spatiotemporal variations are shown in Table 2 and Figure 2a–e. The concentration ranges of these metals in seawater were as follows: Cu (0.50–4.73 μg L^{-1}), Zn (0.34–2.67 μg L^{-1}), Co (0.02–0.16 μg L^{-1}), Ni (0.57–4.36 μg L^{-1}), and Fe (0.02–2.15 μg L^{-1}) (Table 2). Dissolved Cu concentrations within the protected area stations (MPA-1 and MPA-2) ranged from 0.54 to 4.73 μg L^{-1} (Table 2). Overall, the dissolved Cu concentrations were low to moderate across most stations. However, relatively high concentrations were recorded on two occasions, particularly at MPA-1 (3.30–4.73 μg L^{-1}) and MPA-2 (4.40–4.50 μg L^{-1}), followed by MPA-3 (2.71–2.87 μg L^{-1}) during February 2019 and March 2020. Spatially, the highest mean dissolved Cu concentrations were recorded within the MPAs at MPA-2 (1.57 ± 0.93 μg L^{-1}) and MPA-1 (1.53 ± 0.87 μg L^{-1}), followed by MPA-3 (1.42 ± 0.58 μg L^{-1}) near the Doha power and desalination plant outfall. The mean concentration was slightly lower at MPA-5 in Kuwait Bay (1.27 ± 0.36 μg L^{-1}), while the lowest mean concentration was observed at MPA-4 (1.12 ± 0.20 μg L^{-1}), located near the Al-Gazali sewer outlet (Table 2). Seasonally, MPA-1 and MPA-2 exhibited the highest mean concentrations of dissolved Cu during winter, followed by MPA-3 (Figure 2a). Stations MPA-4 and MPA-5 exhibited similar seasonal and spatial patterns (Figure 2a).

Table 2. Comparison of metal concentrations (μg L^{-1}) in the seawater samples of the present study with other studies.

Area of Study	Cu	Zn	Co	Ni	Fe	Reference
MPA1 Within MPA	0.66–4.73 (1.53 ± 0.87)	0.40–2.67 (1.03 ± 0.56)	0.03–0.16 (0.07 ± 0.04)	0.69–3.26 (1.51 ± 0.68)	0.03–2.11 (0.24 ± 0.42)	This study
MPA 2 Within MPA	0.54–4.51 (1.57 ± 0.93)	0.45–1.96 (0.98 ± 0.43)	0.03–0.12 (0.07 ± 0.03)	0.82–4.36 (1.63 ± 0.85)	0.03–2.15 (0.31 ± 0.57)	
MPA-3	0.54–2.87 (1.42 ± 0.58)	0.50–2.76 (0.98 ± 0.55)	0.02–0.16 (0.06 ± 0.03)	0.77–2.72 (1.46 ± 0.61)	0.02–1.10 (0.20 ± 0.0.7)	
MPA-4	0.52–1.73 (1.12 ± 0.30)	0.41–1.89 (0.84 ± 0.32)	0.02–0.13 (0.05 ± 0.02)	0.57–2.16 (1.17 ± 0.44)	0.02–1.36 (0.31 ± 0.33)	
MPA-5	0.50–1.93 (1.27 ± 0.36)	0.34–1.56 (0.72 ± 0.35)	0.02–0.08 (0.05 ± 0.02)	0.61–2.52 (1.22 ± 0.46)	0.03–1.84 (0.32 ± 0.36)	
Kuwait Coast	0.60–2.20	3.60–9.40	-	1.20–4.70	-	[39]
Kuwait Coast	1.82–3.86	1.58–7.16	0.07–1.66	0.18–2.55	4.12–8.94	[40]
Sulaibikhat Bay, Kuwait	0.70–20.0 (4.23)	10.0–98.0 (36.11)	-	BDL–5.0 (0.8)	50.0–120.0 (100.0)	[41]
Sulaibikhat and Kuwait Bay	0.65–1.48	0.33–1.65	0.03–0.08	0.83–1.45	0.04–1.57	[21]
Kuwait Bay	0.95	0.95	0.04	1.31	-	[42]
Mina Al Ahmadi, Kuwait	1.00–9.00	10.00–12.00	BDL–3.00	3.00–6.00	BDL	[43]
Kuwait Bay	235.78–732.03	29.87–538.42	1.03–7.10	63.36–139.29	540.80–2417.50	[44]
Kuwait Coast	-	0–1860.00	-	1730.00–4240.00	-	[45]
MPA, Bangladesh	10.40–56.40	2.90–48.20	-	1.70–16.60	242.40–725.50	[4]
Tisa Lake, Romania	1.60–15.40	9.40–191.30	-	1.30–131.90	22.00–5355.00	[46]
USEPA CWQC USEPA AWQC	3.10 4.80	81.00 90.00	- -	8.20 74.00	- -	[47]
EPA Kuwait OSPAR EAC	15.50 0.01–0.05	- 0.50–5.00	- -	20.00 -	91.30 -	[47]

USEPA Chronic Water Quality Criteria (USEPA CWQC); USEPA Acute Water Quality Criteria (USEPA AWQC); OSPAR Ecotoxicological Assessment Criteria Ranges (OSPAR EAC). Values in parentheses are Mean or Mean ± SD; BDL—Below Detection Limit.

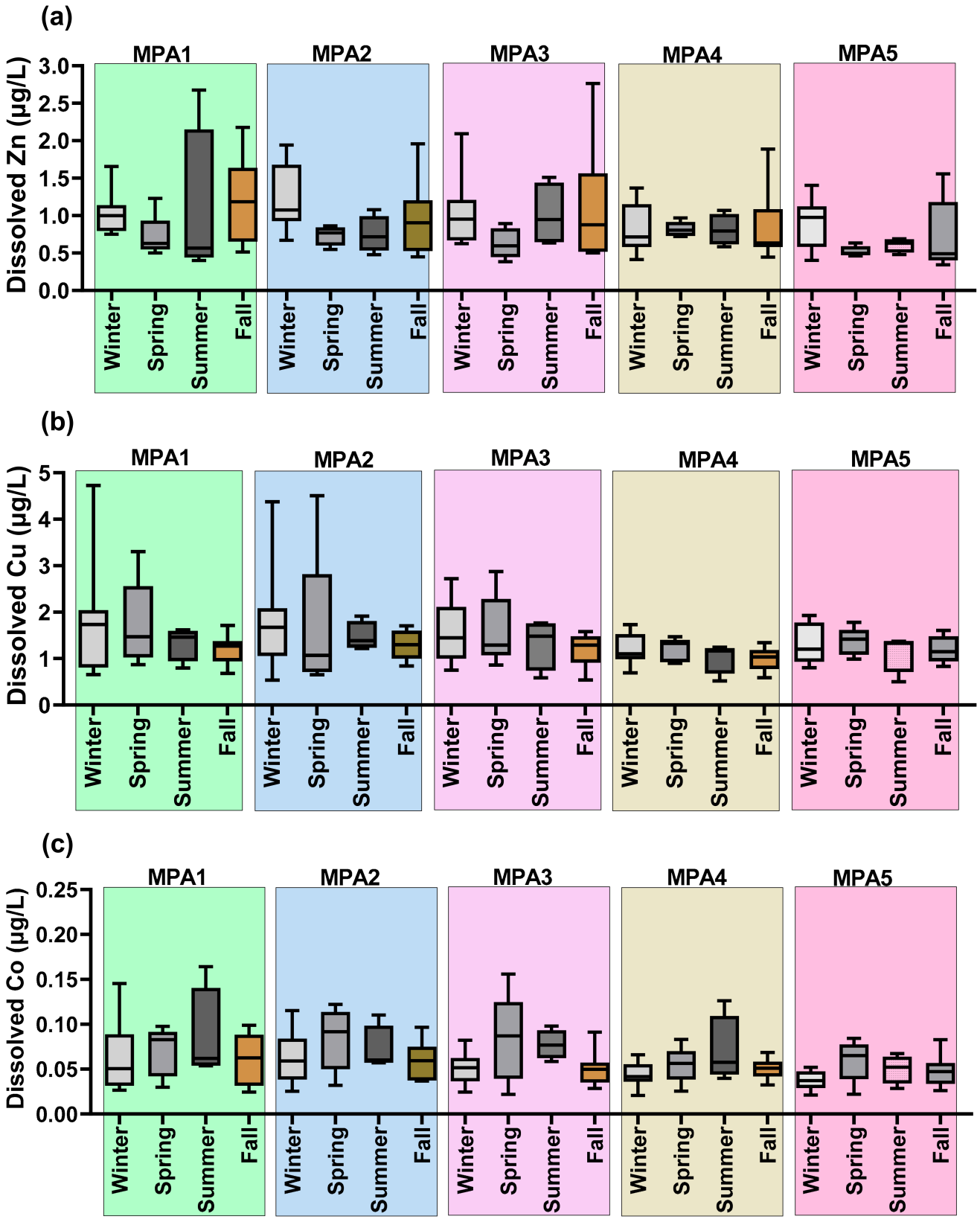


Figure 2. *Cont.*

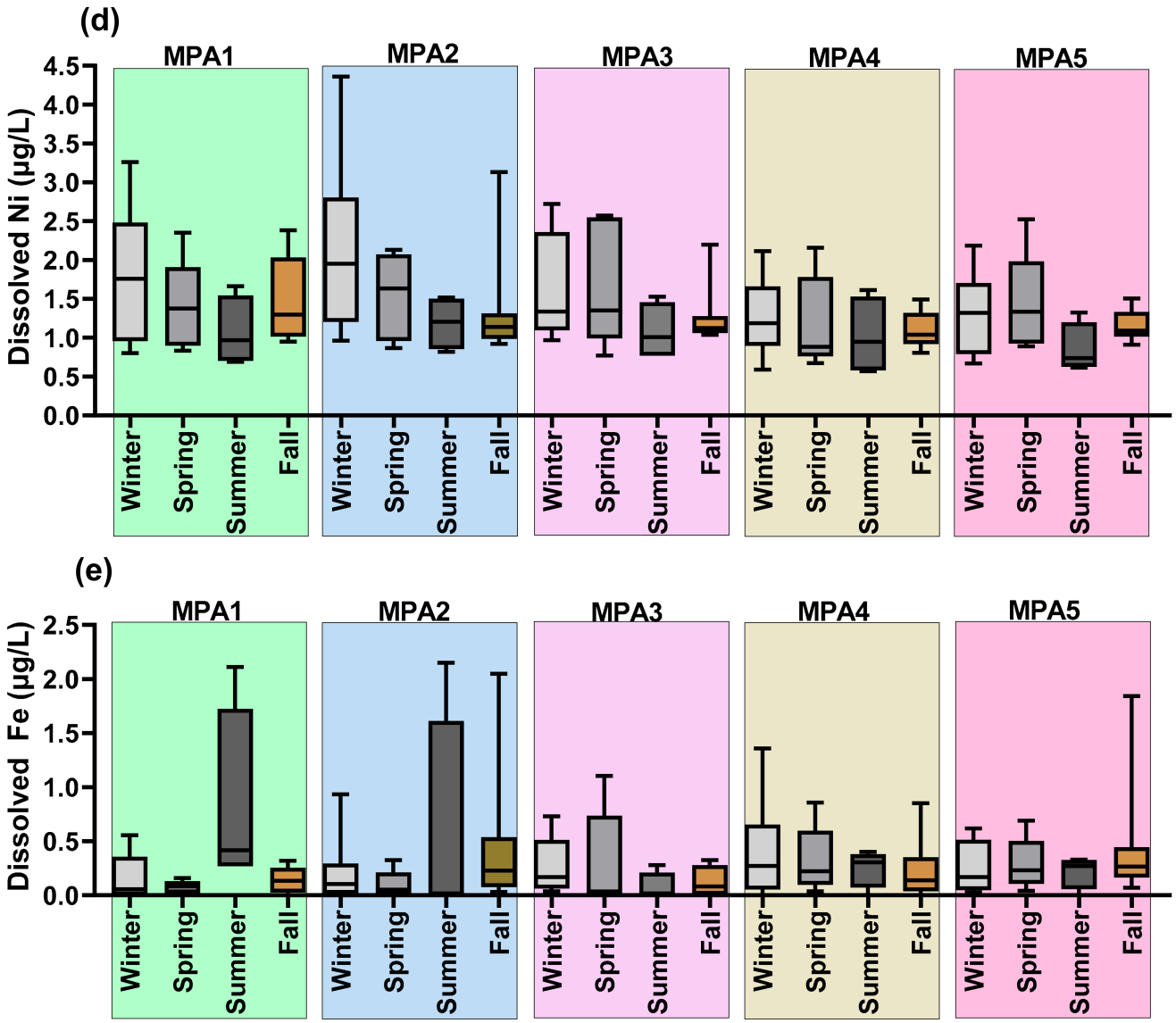


Figure 2. Spatio-temporal variation in Copper (**a**), Zinc (**b**), Cobalt (**c**), Nickel (**d**) and Iron (**e**) in the surface water collected from Sulaibikhat Bay-MPA stations over 26 months from October 2018 until March 2021.

The dissolved Zn concentrations in and around the MPA ranged from 0.34 to 2.76 µg L^{-1} (Table 2). The lowest concentration was observed at MPA-5 in September 2020 (0.34 µg L^{-1}), whereas the highest concentration (2.76 µg L^{-1}) was observed at MPA-3 in October 2018, followed by MPA-1 in June 2019 (2.67 µg L^{-1}). Spatially, the highest mean dissolved Zn concentration was recorded at MPA-1 with an average of 1.03 ± 0.56 µg L^{-1} (Table 2). Mean concentrations at MPA-2 and MPA-3 were similar, each averaging 0.98 ± 0.48 µg L^{-1}. Lower mean concentrations were observed at MPA-4 (0.84 ± 0.32 µg L^{-1}), while the lowest was recorded at MPA-5 (0.72 ± 0.35 µg L^{-1}) (Table 2). Seasonally, MPA-1 exhibited elevated Zn concentrations during fall (1.3 µg L^{-1}), followed by winter (1.03 µg L^{-1}) (Figure 2b). In contrast, summer and spring showed no marked difference, with mean concentrations of 0.81 µg L^{-1} and 0.89 µg L^{-1}, respectively. A similar seasonal pattern was observed at MPA-2, MPA-3, and MPA-5, although at lower concentrations. At MPA-4, Zn concentrations were highest during fall (0.94 µg L^{-1}) and lowest during summer (0.76 µg L^{-1}), whereas winter and spring showed comparable concentrations (0.83 µg L^{-1}) (Figure 2b).

Unlike Cu and Zn, dissolved Co concentrations were consistently low across the study area, ranging from 0.02 to 0.16 μg L^{-1} (Table 2). The highest concentration was recorded at MPA-1 during the summer of 2019, followed by MPA-3 in spring 2019 and MPA-1 in January 2019 (Figure 2c). Seasonally, the mean dissolved Co concentrations at MPA-1, MPA-2, and MPA-3 were slightly higher during spring (0.08 μg L^{-1}), whereas comparable concentrations were recorded during the remaining seasons (Figure 2c). In contrast, lower and relatively uniform mean concentrations were recorded at MPA-4 and MPA-5 (0.05 ± 0.02 μg L^{-1}).

A wide range of dissolved Ni concentrations was observed across the sampling stations (Table 2). The lowest Ni concentration (0.57 μg L^{-1}) was recorded at MPA-4 in February 2019, whereas the highest (4.36 μg L^{-1}) was recorded at MPA-2 in January 2020. At MPA-1, mean dissolved Ni concentrations were highest during winter (1.78 ± 0.85 μg L^{-1}), followed by fall (1.49 ± 0.56 μg L^{-1}). Lower mean concentrations were observed during spring (1.39 ± 0.59 μg L^{-1}) and the lowest during summer (1.07 ± 0.45 μg L^{-1}). A comparable seasonal pattern was observed at MPA-2 and MPA-5. In contrast, MPA-3 showed elevated mean Ni concentrations during winter and spring (1.66 ± 0.67 μg L^{-1}), followed by fall (1.27 ± 0.38 μg L^{-1}) and summer (1.08 ± 0.27 μg L^{-1}). A similar seasonal pattern was observed at MPA-4 (Figure 2d).

Among the bioessential trace metals investigated, Fe exhibited a distinct spatial and seasonal variability. Dissolved Fe concentration ranged from 0.02 to 2.15 μg L^{-1} across all sampling stations (Table 2). The highest concentration was recorded at MPA-1 and MPA-2 (2.15 μg L^{-1}) in June 2019, followed by MPA-4 (1.36 μg L^{-1}) in December 2018, and MPA-3 (1.10 μg L^{-1}) in March 2019 (Figure 2e). Stations MPA-1 and MPA-2, located within the MPA, exhibited the highest mean dissolved Fe concentrations during summer (0.80 μg L^{-1} and 0.53 μg L^{-1}, respectively), whereas the lowest mean values were observed in spring (0.07 μg L^{-1}). Intermediate Fe levels were observed at both stations in winter and fall. At station MPA-3, the highest mean concentrations were observed in winter and spring (0.30 μg L^{-1}), while the lowest mean concentration occurred in summer (0.06 μg L^{-1}). Station MPA-4 had a similar seasonal pattern. In contrast, MPA-5 exhibited a distinct seasonal trend. The highest mean dissolved Fe concentration was recorded during fall (0.45 μg L^{-1}), whereas lower mean concentrations were observed (0.24 μg L^{-1}) during other seasons (Figure 2e).

To place these observations in broader environmental context, the measured concentrations were compared with previously reported values from Kuwait and other marine protected areas, other regions, and relevant regulatory standards (Table 2). The measured concentrations in this study were low to moderate, likely reflecting the combined influence of natural geochemical and localised anthropogenic inputs. Spatially, higher mean concentrations were observed at stations within the Sulaibikhat MPA (MPA-1 and MPA-2) and near the Doha power and desalination plant outfall (MPA-3), suggesting the influence of land-based discharge and restricted water circulation in the bay at these stations [28]. The observed values were comparable to those reported by Al Said et al. [21] for Kuwait Bay, including Sulaibikhat Bay (Table 2). However, several studies reported significantly higher concentrations of Cu, Zn, Ni, and Fe in Sulaibikhat Bay compared to the present study (Table 2) [41,44,45]. The occasional increases recorded during fall may be linked to atmospheric wet deposition and flash flood events, whereas the higher summer concentrations may be due to atmospheric dry deposition associated with increased dust inputs. Aeolian dust from this region is recognised as a rich source of trace elements, especially Fe [48,49]. The concentrations of dissolved trace metals observed in this study were lower than those reported for marine protected areas in Bangladesh and protected lakes of Romania (Table 2). Comparison of observed concentrations in the Sulaibikhat

MPA with established marine water quality criteria showed that Cu, Zn, and Ni remained well below the USEPA acute and chronic thresholds and the Kuwait EPA limits (Table 2). Although Zn concentrations were below the OSPAR ecotoxicological assessment criteria (OSPAR EAC), Cu concentrations exceeded these criteria, indicating a potential ecological risk to the Sulaibikhat Bay system.

3.2. Metal Composition of the Surface Sediments

Sediments play an important role in controlling the distribution of trace metals in the marine environment. After entering coastal waters, metals bind to fine particles and organic matter, then settle to the bottom, making sediments the main sink for these contaminants [50]. Changes in physicochemical conditions, including redox potential, pH, and hydrodynamic disturbances, may promote the remobilisation of sediment-bound metals, thereby enhancing their bioavailability. This may pose long-term risks to benthic communities and facilitate the transfer of metals through the food web, ultimately reaching humans via bioaccumulation and biomagnification [11,16,17,50]. Therefore, evaluating sediment contamination is crucial for assessing ecological risks and historical pollution patterns, allowing the identification of contaminant sources, characterisation of dispersal pathways, and detection of temporal and spatial trends. Analyses of surface sediments provide insights into current ecological conditions, forming the basis for environmental management, ecological risk assessment, and regulatory decision-making [10].

The mean concentrations (±SD) of 17 metals analysed in sediments collected from stations within and around the Sulaibikhat MPA across all seasons are shown in Table 3. These values were compared with those reported in previous studies from Kuwait and other marine protected regions to provide a regional and global context for evaluating natural enrichment and anthropogenic influences (Table 4). Among the 17 elements studied, surface sediments showed relatively higher concentrations of major lithogenic components, including Al, Fe, Ti, and Mn. The mean concentrations of Al and Fe were highest at MPA-1 to MPA-4 and declined sharply at MPA-5 (Table 3). A similar trend was observed for other metals, including Ti, Co, and Mn. The higher concentrations of these elements at stations within Sulaibikhat Bay, especially near the Al-Gazali sewer outlet, are consistent with terrigenous input and fine-grained sediment deposition in semi-enclosed coastal embayments. In contrast, the comparatively lower concentrations of these elements at MPA-5, located outside Sulaibikhat Bay, could be attributed to its coarse-sandy substrate. Despite these spatial differences, the concentrations of all measured metals remained below the UCC reference values. Lower concentrations of Fe and Al have been reported from MPAs in northern Brazil and the northern Persian Gulf, Iran [5,8]. However, the spatial distribution pattern observed in the present study is consistent with earlier studies from Kuwait Bay and similar coastal environments, where sediment composition is strongly controlled by natural mineralogy and catchment-derived materials [51,52]. These findings suggest that the abundance of major lithogenic elements in the Sulaibikhat Bay MPA is primarily associated with the geological background rather than anthropogenic contamination.

Table 3. The mean concentrations (μg g^{-1}) of 17 elements in sediments from the first marine protected area of the northwestern Arabian Gulf.

Location	Sr	Mo	Cd	Ba	Pb	Th	U	Al	Ti	V	Cr	Mn	Fe	Co	Ni	Cu	Zn
MPA 1	426.6 ± 32.7 ^{a}	1.4 ± 0.3 ^{b}	0.6 ± 0.2 ^{a}	176.7 ± 7.3 ^{b}	11.4 ± 0.4 ^{c}	4.1 ± 0.1 ^{b}	2.2 ± 0.0 ^{ab}	42,898.8 ± 1531.9 ^{b}	3008.1 ± 104.1 ^{b}	103.4 ± 4.6 ^{c}	209.5 ± 11.6 ^{b}	554.9 ± 30.4 ^{b}	29,215.6 ± 1007.9 ^{b}	17.0 ± 0.5 ^{b}	134.9 ± 12.1 ^{bc}	59.5 ± 7.0 ^{d}	94.9 ± 5.2 ^{cd}
MPA 2	453.7 ± 26.4 ^{a}	1.1 ± 0.1 ^{ab}	0.5 ± 0.0 ^{a}	180.7 ± 9.7 ^{b}	9.8 ± 0.3 ^{b}	3.4 ± 0.4 ^{b}	1.9 ± 0.1 ^{a}	36,160.1 ± 4791.3 ^{b}	2760.9 ± 36.8 ^{b}	86.8 ± 2.4 ^{b}	216.3 ± 13.2 ^{b}	532.7 ± 16.8 ^{b}	24,998.8 ± 900.2 ^{b}	14.8 ± 0.6 ^{b}	111.2 ± 5.0 ^{b}	36.2 ± 2.6 ^{b}	68.9 ± 4.0 ^{b}
MPA 3	461.2 ± 48.1 ^{a}	1.4 ± 0.3 ^{b}	0.6 ± 0.2 ^{a}	185.2 ± 16.8 ^{b}	10.6 ± 0.9 ^{bc}	3.8 ± 0.4 ^{b}	2.1 ± 0.2 ^{ab}	40,589.0 ± 3319.5 ^{b}	2904.4 ± 241.4 ^{b}	94.2 ± 5.9 ^{bc}	230.1 ± 56.7 ^{b}	556.1 ± 47.5 ^{b}	26,803.8 ± 1894.5 ^{b}	15.7 ± 1.2 ^{b}	118.3 ± 7.2 ^{b}	48.2 ± 2.0 ^{c}	84.3 ± 3.7 ^{c}
MPA 4	435.4 ± 51.2 ^{a}	1.5 ± 0.1 ^{b}	0.7 ± 0.1 ^{a}	181.3 ± 21.4 ^{b}	13.4 ± 1.2 ^{d}	4.4 ± 0.6 ^{bc}	2.4 ± 0.3 ^{b}	44,722.8 ± 6271.8 ^{bc}	3189.3 ± 392.7 ^{b}	110.5 ± 12.9 ^{c}	192.9 ± 37.5 ^{b}	604.9 ± 68.9 ^{b}	33,026.2 ± 3701.9 ^{c}	18.7 ± 2.2 ^{c}	142.6 ± 16.3 c	48.9 ± 4.2 ^{c}	97.8 ± 10.0 ^{d}
MPA 5	4382.5 ± 50.7 ^{b}	0.8 ± 0.2 ^{a}	0.4 ± 0.0 ^{a}	67.8 ± 2.4 ^{a}	5.2 ± 0.2 ^{a}	1.1 ± 0.0 ^{a}	2.4 ± 0.4 ^{b}	10,670.6 ± 600.9 ^{a}	734.1 ± 55.7 ^{a}	31.5 ± 0.4 ^{a}	62.4 ± 17.6 ^{a}	175.7 ± 10.5 ^{a}	8340.4 ± 878.4 ^{a}	4.3 ± 0.3 ^{a}	30.9 ± 0.7 ^{a}	11.5 ± 0.4 ^{a}	22.1 ± 3.2 ^{a}
UCC	320	1.1	0.10	628	20.0	10.5	2.7	81,500	N/A	97	92	600	39,200	17.3	47	28	67

Sr—Strontium, Mo—Molybdenum, Cd—Cadmium, Ba—Barium, Pb—Lead, Th—Thorium, U—Uranium, Al—Aluminium, Ti—Titanium, V—Vanadium, Cr—Chromium, Mn—Manganese, Fe—Iron, Co—Cobalt, Ni—Nickel, Cu—Copper and Zn—Zinc. UCC—The Earth's upper continental crust (UCC) of different metals is taken from Rudnick and Gao [31]. Values are mean ± SD (n = 8). The letters a, b, c, and d represent significant differences between elements at different stations (same letters not significant); N/A—Not Available.

Table 4. Comparison of metal concentrations (μg g^{-1}) of sediments from the present study with those of different marine protected areas worldwide.

Study Area	Al *	Ba	Cd	Cr	Co	Cu	Fe *	Pb	Mn	Mo	Ni	Sr	Th	Ti	U	V	Zn	References
MPA1	41,448.30–44,659.10	168.70–188.20	0.33–0.79	196.10–224.50	16.70–17.60	49.30–69.30	28,141.00–30,285.00	11.00–11.90	508.20–585.70	1.00–1.70	126.20–155.20	376.00–458.20	3.90–4.30	2888.30–3071.10	2.20–2.30	96.40–108.60	86.70–100.10	This study
MPA 2	27,611.40–38,615.10	167.60–193.50	0.43–0.50	202.80–226.50	13.80–15.60	31.90–38.20	23,508.30–25,694.70	9.30–10.00	520.40–560.80	0.90–1.20	102.60–115.10	430.70–499.10	2.70–3.60	2723.60–2804.80	1.80–2.10	82.70–89.00	63.50–74.40	
MPA3	36,658.10–45,610.70	162.10–206.00	0.39–0.77	183.70–325.50	14.60–17.40	45.20–50.30	24,566.60–29,279.30	9.70–11.60	504.30–621.70	1.10–1.80	111.80–130.30	398.20–502.80	3.40–4.40	2615.80–3230.20	2.00–2.20	87.70–102.30	80.40–89.10	
MPA4	39,508.40–54,689.70	161.80–212.40	0.58–0.77	161.50–241.80	16.90–22.30	45.20–55.40	30,107.50–38,925.50	12.60–15.40	510.00–686.50	1.40–1.60	128.59–168.30	377.00–511.80	3.70–5.40	2885.30–3824.50	2.10–2.80	98.50–131.30	88.00–112.40	
MPA5	10,025.50–11,214.60	66.10–70.50	0.36–0.39	46.90–81.50	3.20–4.60	11.06–11.79	7501.40–9253.40	5.00–5.30	167.90–187.60	0.60–1.00	30.15–31.48	3840.50–4878.90	1.10–1.10	690.20–796.80	2.00–2.70	31.10–31.80	20.20–25.80	

Table 4. *Cont.*

Study Area	Al *	Ba	Cd	Cr	Co	Cu	Fe *	Pb	Mn	Mo	Ni	Sr	Th	Ti	U	V	Zn	References
Studies from Kuwait																		
Sulaibikhat Bay	-	-	4.40–6.10	19.10–40.40	17.30–24.50	5.50–36.10	4018.10–10,200.00	<1	1.20–1.50	<1	42.10–125.30	-	-	-	<1	29.30–32.60	18.00–225.20	[22]
Kuwait Bay & Sulaibikhat Bay	-	-	<0.20–0.50	108.20–429.00	-	-	-	9.70–33.20	-	-	86.20–169.30	-	-	-	-	-	66.50–140.70	[23]
Kuwait Bay	-	-	-	27.00–87.60	2.20–17.30	3.20–21.20	-	2.60–9.00	-	-	19.80–82.10	-	-	-	-	-	10.60–78.00	[53]
Sulaibikhat Bay	-	-	2.00–4.00	68.00–206.00	3.90–23.60	10.90–108.00	-	2.40–36.20	-	-	28.80–128.00	-	-	-	-	-	18.60–310.00	[54]
Sulaibikhat Bay	-	-	8.40–10.30	17.00–170.30	-	17.10–93.30	1073.50–29,339.00	16.80–44.30	45.40–512.50	-	15.50–115.80	-	-	-	-	37.70–423.10	9.20–389.40	[55]
Kuwait Bay	1823.00–89,501.00	20.10–41.10	<0.08–2.90	47.10–83.50	8.10–15.70	1.40–40.70	8982.00–15,257.00	<0.70–2.90	247.70–412.60	–	56.60–103.40	–	–	–	–	20.30–44.50	3.40–73.00	[51]
Kuwait Bay	-	-	0–0.42	12.40–70.60	0–5.50	3.60–21.30	-	0–33.00	-	-	3.70–32.20	-	-	-	-	15.80–74.20	11.20–68.20	[56]
Kuwait Bay	4000.00–69,000.00	-	0–0.40	2.30–71.00	0–6.20	0–40.10	2000.00–39,000.00	0–33.00	-	-	0–32.30	-	-	-	-	4.10–74.20	3.40–73.00	[52]
Studies from MPAs across the World																		
Protected lakes, Poland	-	-	0.00–7.60	2.50–106.00	-	0.20–164.00	-	2.00–150.00	-	-	1.30–29.00	-	-	-	-	-	13.00–240.00	[57]
Sangomer MPA, Senegal	-	-	0–37.20	-	-	-	-	0–5.20	-	-	-	-	-	-	-	-	-	[6]
Kosterhavet National Park (MPA), Sweden	-	-	0.10–0.20	-	-	15.0–20.0	-	20.0–35.0	-	-	24.0–32.0	-	-	-	-	-	95.0–125.0	[58]
CIP Protected Area, Brazil	411.0–13,630.0	-	0.00–0.20	0.40–32.00	0.40–10.0	0.0–16.30	907.0–26,661.0	0.80–40.20	16.10–221.20	-	0.30–11.70	-	-	-	-	-	1.70–45.20	[59]
CIP Protected Area, Brazil	-	-	<0.10–13.10	<0.10–280.00	-	0.0–292.0	-	0.30–247.0	-	-	-	-	-	-	-	-	1.40–176.0	[60]

Table 4. *Cont.*

Study Area	Al *	Ba	Cd	Cr	Co	Cu	Fe *	Pb	Mn	Mo	Ni	Sr	Th	Ti	U	V	Zn	References
North Shore MPA, Brazil	0.50–2.40%	-	0.20–0.90	6.10–17.70	-	2.60–19.0	0.60–2.40%	2.80–10.70	-	-	2.10–7.10	-	-	-	-	-	12.50–54.80	[8]
MPA, Bali, Indonesia	-	-	-	13.2–22.0	4.2–6.4	-	26,500–32,500	-	-	-	-	-	-	-	-	-	46.0–72.3	[10]
Northern Persian Gulf MPAs, Iran	0.80–4.10%	-	BDL	39.0–142.0	2.0–12.0	4.0–20.0	0.40–1.60%	7.0–459.0	184.0–425.0	BDL	18.0–90.0	-	-	-	-	15.0–58.0	6.0–424.0	[5]
Antarctic Protected Area 161 **	-	-	ND–7.90	-	-	0.60–50.20	-	ND–17.60	-	-	-	-	-	-	-	-	6.90–45.50	[13]
Caribbean protected area, Colombia	-	-	0.30–0.70	-	-	18.90–45.90	-	1.30–1.90	-	-	-	-	-	-	-	-	50.30–95.00	[61]

* Two studies reported the value as %. ** Reported values are in nanomoles. BDL—Below Detection Limit; ND—Not Detected.

The occurrence and enrichment of Cd, Pb, Cu, Zn, and Ni in coastal sediments are widely used as indicators of anthropogenic contamination. In this study, Mo and Cd levels were generally low across all sites, with Mo ranging from 0.8 ± 0.2 to 1.5 ± 0.1 μg g^{-1} and Cd from 0.4 ± 0.02 to 0.7 ± 0.1 μg g^{-1}. The values for these metals are comparable to, or slightly exceed, the UCC levels (Table 3). The Cd concentrations observed across the study area are comparable to those reported by Lyons et al. [23] but lower than those reported for Kuwait Bay, including Sulaibikhat Bay [22,51,54,55]. Cd concentrations were higher than those reported for Kosterhavet National Park in Sweden (0.05–0.15 μg g^{-1}) and Brazilian protected areas (0.0097–0.17 μg g^{-1}), but lower than those for different MPAs in West Africa, Brazil, Poland, and Antarctica [6,13,57,60]. Although Cd concentrations were lower than those in earlier studies, the semi-enclosed Sulaibikhat Bay remains influenced by anthropogenic pollution sources, including industrial and urban wastewater discharge, maritime activities, and legacy contamination.

Evidence of these influences is further reflected in the distribution of transition metals. Among the transition metals, V, Ni, and Cr concentrations in the sediments were higher within (MPA-1 and MPA-2) and around the Sulaibikhat Bay MPA (MPA-3 and MPA-4) and lower at the Kuwait Bay reference station (MPA-5), located outside the MPA (Table 3). The observed values were comparable to those reported for sediments from the Northern Persian Gulf but were higher than those reported for protected lakes in Poland and some Brazilian MPAs (Table 4). Generally, Ni and V are known as geochemical tracers of petroleum-derived inputs [15,62]. The elevated V concentrations in the Sulaibikhat Bay system are consistent with earlier findings reported by Alshraifi et al. [55]. The enrichment of Cr, Ni, and V relative to the UCC values in Sulaibikhat Bay indicates potential contributions from hydrocarbon-related activities, industrial discharges, and harbour operations within this intensively used coastal embayment.

Additional evidence of anthropogenic influence is provided by the distribution of Cu and Zn, which are associated with urban and maritime activities. Cu and Zn are associated with antifouling paints, industrial discharges, and municipal wastewater. They were comparatively higher at stations MPA-1 to MPA-4 than at MPA-5 (Table 3). Although these concentrations exceeded those reported for several MPAs worldwide (Table 4), Zn concentrations were within the range reported for other marine protected regions, such as Bali mangrove sediments (46–72 μg g^{-1}) [10] and Caribbean protected areas (50–95 μg g^{-1}) [61]. However, previous studies in Sulaibikhat Bay have reported much wider ranges, with Cu reaching 108 μg g^{-1} [54] and Zn reaching 389 μg g^{-1} [55], indicating pronounced spatial heterogeneity and temporal variability in contamination levels, likely influenced by sediment characteristics and fluctuating pollution sources.

Unlike Cu and Zi, Pb concentrations at all stations were below the corresponding UCC values and ranged from 5.2 ± 0.2 to 13.4 ± 1.2 μg g^{-1} (Table 3). Pb concentrations were relatively low compared to those reported for several international MPAs, such as the marine protected areas in the northern Persian Gulf, Iran, where Pb concentrations reached 459 μg g^{-1} [5] (Table 4). In addition, earlier studies from Kuwait Bay and Sulaibikhat Bay reported relatively low sediment Pb concentrations (Table 4), suggesting that Pb contamination does not currently pose a major concern in the Sulaibikhat Bay MPA.

The remaining elements studied (Sr, Ba, U, Th) displayed distinct spatial patterns that were largely consistent with natural sediment characteristics rather than anthropogenic enrichment. The mean Sr concentrations at MPA-1 to MPA-4 were approximately tenfold lower than those observed at MPA-5, where concentrations exceeded the corresponding UCC values (Table 3). The mean Ba concentrations at MPA-1 to MPA-4 ranged from 176.7 ± 7.3 to 185.2 ± 16.8 μg g^{-1}, whereas substantially lower levels were recorded at MPA-5

(67.8 ± 2.4 μg g^{-1}). U and Th concentrations were relatively uniform across the stations and remained below the UCC values, suggesting no anthropogenic influence (Table 3).

3.2.1. Spatiotemporal Distribution of Trace Metals in Sediments

The spatial and seasonal distributions of all 17 elements are shown in Supplementary Figure S1a–c. Sediment core collection at MPA-5 was technically challenging due to the sandy substrate. Sediment cores were successfully retrieved in winter, summer, and fall after multiple attempts; however, spring sampling was unsuccessful. The spatial and seasonal variations of Sr, Mo, Cd, Ba, Pb, and Th are presented in Figure S1a.

Sr concentrations were consistently higher, whereas Mo, Cd, Ba, Pb, and Th levels were consistently lower at MPA-5, located in Kuwait Bay, than at the other stations across all sampled seasons. Mo levels were moderately elevated at MPA-4 during most seasons (>1.4 μg g^{-1}) (Figure S1a, panels a–d), except in spring and fall, when the highest concentrations were recorded at MPA-3 (1.63–1.77 μg g^{-1}). During summer, the maximum Mo concentration was observed at MPA-1 (1.67 μg g^{-1}). Similar spatiotemporal patterns were evident for Cd, except during spring, when MPA-1, MPA-3, and MPA-4 showed high Cd levels. At all these stations, the Cd concentrations were 0.7 μg g^{-1} (Figure S1a, panels i–l). Higher Ba levels were observed at all four stations (MPA-1, MPA-2, MPA-3, and MPA-4) within Sulaibikhat Bay, especially in summer and fall. Pb concentrations in surface sediments were consistently highest at MPA-4 across all seasons (12–13 μg g^{-1}), followed by MPA-1 (10–12 μg g^{-1}). Thorium also showed a similar trend, with the highest concentrations recorded at MPA-4 (4.05–5.35 μg g^{-1}).

The spatiotemporal variations in the concentrations of U, Al, Ti, V, Cr, and Mn in surface sediments within and around the MPA are shown in Figure S1b. Uranium concentrations were highest at station MPA-5 (2.02–2.78 μg g^{-1}) across most seasons; however, in fall, the maximum concentration was recorded at MPA-4 (4.58 μg g^{-1}) (Figure S1b).

Al, Ti, V, and Mn also showed similar spatiotemporal patterns, with consistently higher concentrations at MPA-4 and lower concentrations at MPA-5 across all seasons (Figure S1b). In contrast, Cr displayed a distinct distribution pattern, with concentrations exceeding 210 μg g^{-1} at MPA-1, MPA-2, and MPA-3, the latter located near the Doha power and Desalination plant outfall, during all seasons (Figure S1b, panel q–t). Lower Cr concentrations were observed at MPA-4 (160–200 μg g^{-1}), except in fall, when the concentration increased to 220 μg g^{-1}. The lowest Cr concentrations were consistently recorded at MPA-5 (40–80 μg g^{-1}) across all seasons.

Seasonal and spatial distributions of Fe, Co, Ni, Cu, and Zn in surface sediments across the study area are shown in Figure S1c. Fe, Co, Ni, and Zn exhibited a distribution pattern similar to that observed for Pb, with consistently elevated concentrations at MPA-4 (Fe: 30,107.5–38,925.5 μg g^{-1}, Co: 17.8–22.3 μg g^{-1}, Ni: 130.2–168.3 μg g^{-1}, Zn: 90.4–103.04 μg g^{-1}) across all seasons and lowest at MPA-5 (Fe: 7501.4–9253.4 μg g^{-1}, Co: 4.0–4.29 μg g^{-1}, Ni: 30.2–31.5 μg g^{-1}, Zn: 20.2–25.81 μg g^{-1}) (Figure S1c, panels a–l and q–t).

Fe, Co, Ni, and Zn concentrations were generally comparable at the other three stations, except during winter and spring, when MPA-1 showed slightly higher concentrations. In contrast, Cu displayed a distinct spatial pattern with the highest concentrations (50–60 μg g^{-1}) consistently recorded at MPA-1 and the lowest at MPA-5 (11 μg g^{-1}) throughout the study period (Figure S1c, panels m–p). At MPA-2, MPA-3, and MPA-4, Cu concentration ranged from 30 to 50 μg g^{-1}. However, during summer and fall, it was slightly higher at MPA-4 (50.81 μg g^{-1} and 50.64 μg g^{-1}, respectively).

The present study revealed marked spatial heterogeneity in sediment metal distributions among the stations studied. To understand the sources of metal contamination, a

PCA was conducted and is shown in Figure 3. PC-1 explains 90% of the variance, and PC-2 explains 9% (Figure 3).

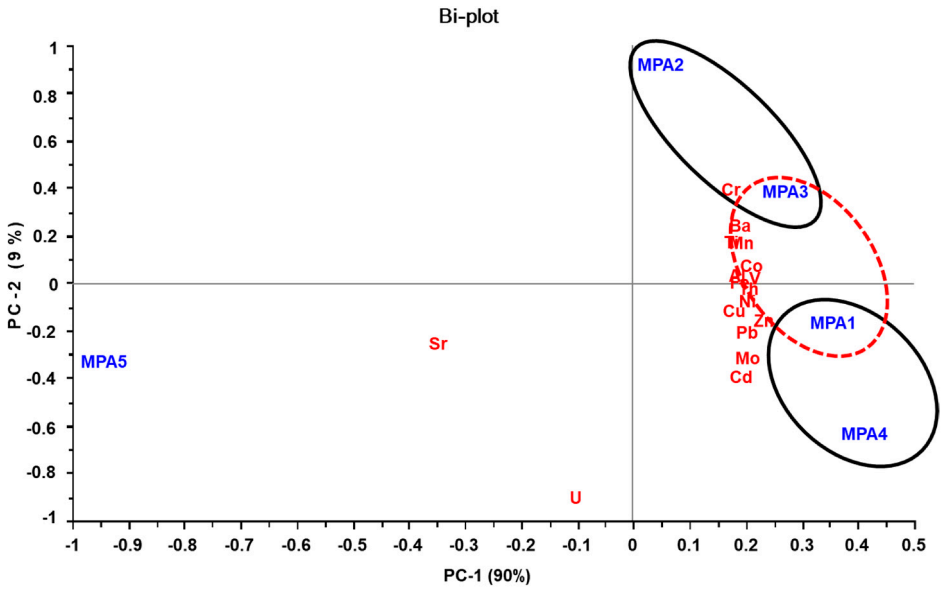


Figure 3. The Biplot of Principal component analysis (PCA) performed on sediment metal composition at different stations, showing the origin of the anthropogenic metal contamination in the marine protected area.

PC-1 separates the sampling stations along an anthropogenic contaminant gradient, whereas PC2 reflects geochemical variability. Stations MPA-1 to MPA-4, with higher metal concentrations and near anthropogenic inputs, are placed on the positive side of PC1. Station MPA-5, the reference station with low metal concentrations, is placed on the negative side of PC1. PC2 groups the stations MPA-3 and MPA-2 in the upper-right corner, where higher Cr concentrations are observed, suggesting an anthropogenic origin with industrial discharges from the nearby power and desalination plants. Similarly, MPA-1 and MPA-4 clustered together in the lower left quadrant of the PCA, corresponding to higher concentrations of Cd, Mo, Pb, and Zn, suggesting their origin mainly from the Al Gazali sewer outlets. A similar pattern of enhanced metal loads near the Al-Ghazali outlet was reported by Alshemmari et al. [54]. Most of the remaining metals clustered around the origin of the PCA plot, indicating relatively similar distributions among MPA-1 to MPA-4 and lower concentrations at MPA-5. The higher concentrations of several metals at MPA-1 than MPA-2 are due to the anthropogenic influence of both Doha power/and Desalination plant effluents (MPA-3) as well as the Al Gazali sewage outlet (MPA-4) (Figure 3). The association of Sr and U with MPA-5 in the negative quadrant of PC-1, away from the anthropogenic pollution source, indicates that it is of natural origin. The strong loading of U in the lower negative regions of both PC-2 and PC-1 further suggests that its distribution is strongly influenced by geochemical processes. These results highlight the influence of localised contamination sources in addition to hydrodynamic and sedimentological conditions on sedimentary metal distributions. Further, the semi-enclosed nature of Sulaibikhat Bay and the predominance of fine-grained sediments may increase the retention and accumulation of trace metals due to low water exchange [27]. In contrast, the coarser sediment type and improved hydrodynamic conditions outside Sulaibikhat Bay (MPA-5) may be less favourable for metal adsorption and accumulation on the bottom sediment. A negative relationship was reported between the sand fraction and trace metal concentrations. Finer sediment components, such as mud and silt, are more effective at retaining

trace elements [54]. Higher silica content in sandy sediments has a lower affinity for trace metals, leading to lower metal binding than in clay-rich fractions [63].

Overall, the PCA results suggest that surrounding land-use activities, particularly wastewater discharges and industrial operations, influence the spatial distribution of trace metals within Sulaibikhat Bay. However, a quantitative watershed-scale land-use analysis was beyond the scope of the present study.

3.2.2. Environmental Contamination Indices

Environmental contamination indices are widely used to evaluate the source, extent and ecological risks of metal accumulation in marine sediments. In this study, an integrated evaluation using the EF, I_{geo}, PLI, and ERI [64] revealed distinct spatial variations and metal-specific contamination patterns within and around the Sulaibikhat Bay MPA.

The EF values for the different metals across the study area are shown in Figure 4a. The EF value indicates the degree of metal enrichment in the environmental samples. The degree of enrichment can be interpreted using EF values, where <2 indicates minimal enrichment, 2–5 indicates moderate enrichment, and 5–20 indicates significant enrichment. EF values of 20–40 indicate a very high level of enrichment, whereas values > 40 indicate extremely high enrichment [30]. Based on these classifications, Ba, Pb, Al, V, Mn, Fe, Co, and Zn showed minimal to no enrichment at all stations (Figure 4a). However, Sr showed moderate enrichment at MPA-2 and extremely high enrichment at MPA-5. Mo and U were moderately enriched at MPA-5, whereas all other stations were at background levels. Cr and Ni were moderately enriched at all stations, whereas Cu was moderately enriched only at MPA-1 and MPA-3.

$I_{geo,}$ values were determined for multiple metals in sediments from all five stations to assess historical metal contamination (Figure 4b). I_{geo} values classify sediment quality as unpolluted ($\leq$0), unpolluted to moderately polluted (0–1), moderately polluted (1–2), moderately to heavily polluted (2–3), heavily polluted (3–4), heavily to extremely polluted (4–5), and extremely polluted (>5) [30]. Based on this criterion, there was no threat of metal pollution from Mo, Ba, Pb, Th, U, Al, V, Mn, Fe, and Zn at any of the five stations (Figure 4b). Although Sr posed no pollution threat at MPA-1 to MPA-4, MPA-5 showed an I_{geo} value greater than 3, indicating heavy contamination. Cd levels suggested moderate to heavy pollution at all stations, with I_{geo} values ranging from 1.38 to 2.39. Except for MPA-5, surface sediments at all other stations were classified as moderately to heavily polluted with respect to Cr and Ni (Figure 4b). For MPA-1, MPA-3, and MPA-4, the I_{geo} values of Cu ranged from 0.27 to 0.88, placing these stations in the unpolluted to moderately polluted category (Figure 4b).

The geogenic or anthropogenic origin of the metal pollution in sediments can be assessed by the enrichment factor (EF). The I_{geo} complements EF by reflecting the historical accumulation of metals relative to background or pre-industrial levels, thereby indicating the severity of sediment contamination. EF and I_{geo} results showed that most metals, including Ba, Pb, Al, V, Mn, Fe, Co, and Zn, had EF values below 2 and I_{geo} values $\leq$ 0 across the study area, indicating a predominantly lithogenic origin of these metals. The low enrichment of these conservative elements may be attributed to the aluminosilicate minerals and natural sedimentary inputs rather than to human activities [65,66]. However, Cu showed low to moderate enrichment (EF: 1.9–2.79) and moderate pollution (I_{geo}: 0.39–0.56) at stations MPA-1, MPA-3, and MPA-4, which are likely due to the localised inputs from power-desalination plants, maritime activities, and urban runoff.

Cr and Ni showed moderate enrichment (EF 2–5) at all stations, including MPA-5, suggesting contributions from both lithogenic and anthropogenic sources. These patterns have been reported in coastal sediments affected by petroleum-related activities and industrial discharges, especially in regions with intensive oil exploration and shipping traffic [23,67].

Specifically, Ni is an important metallic constituent of crude oil and is detected at higher concentrations in oil-producing regions than in non-petroleum areas [68]. Cd was significantly enriched in all stations, indicating widespread contamination. Cd is considered the most hazardous, toxic and carcinogenic [69]. The presence of high Cd levels in coastal sediments is of concern due to their environmental persistence and strong association with sources of pollution, such as industrial effluents, phosphate fertilisers, antifouling coatings, and petroleum-related activities [69]. Their accumulation in sediments poses a significant threat to benthic organisms, alters microbial community structure, and impairs overall ecosystem stability [18,70]. The I_{geo} values for Cd, Cr, and Ni were in the moderate to high pollution range at stations MPA-1 to MPA-4 in Sulaibikhat Bay, correlating with anthropogenic inputs at these stations.

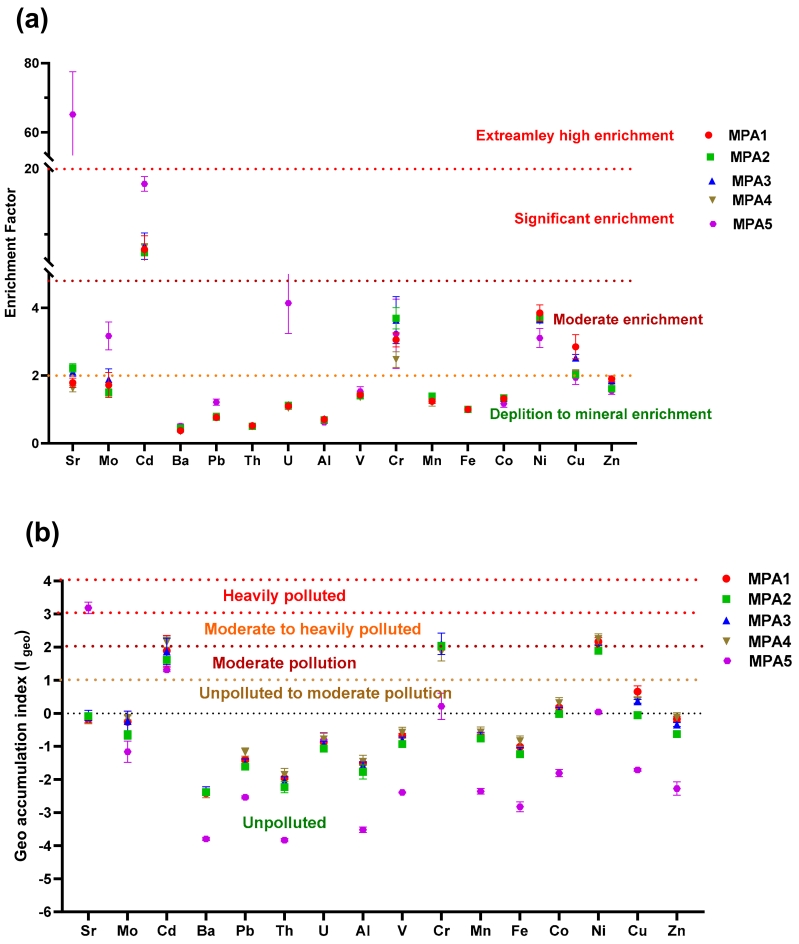


Figure 4. Enrichment factor (**a**) and the geoaccumulation index (I_{geo}) (**b**) of the different metals in and around the marine protected area.

The very high EF and I_{geo} value (more than 3) for Sr at station MPA-5 suggested heavy enrichment relative to historical background levels. Usually, higher Sr levels in marine sediments are linked to biogenic carbonates rather than indicating direct anthropogenic inputs [71]. The selective enrichment of Sr relative to other studied metals at MPA-5 and the presence of coarse sediment characteristics may be due to local sedimentary conditions or the possible presence of carbonate-rich deposits. In addition, biogenic components, such as foraminiferal tests, coccolithophores, and shell fragments, also might have contributed to higher Sr in MPA-5 [71].

The moderate enrichment of Mo and U at MPA-5 is affected by redox-sensitive processes and sediment mineralogy, especially in environments with limited oxygen conditions [72]. Mo and U are usually low in continental crust, stable under oxic conditions, and

exhibit long residence times in seawater. These properties make Mo and U concentrations uniform in global seawater and make them useful indicators of paleoenvironmental conditions [72,73]. The concentrations of Mo and U in plankton are generally low, and hence their enrichment in sediments may be due to authigenic uptake from seawater [72]. Station MPA-5 was the deepest site examined in this study (4.4 m) compared with all other stations (2–3 m). The observed enrichment at station MPA-5 may be associated with depth-related redox variations. The higher EF values for U than for Mo indicate differences in their geochemical behaviour under an oxygen-depleted state. Uranium deposition in sediments is initiated under low-oxygen conditions at the Fe redox boundary and is enhanced in sulfide-rich environments, before Mo accumulation [74–76]. Mo enrichment in sediments is promoted by Mn–Fe oxyhydroxide particle transport, a mechanism that does not influence U accumulation [77]. Different uptake pathways for Mo and U provide valuable insights into the prevailing geochemical conditions in MPA-5, where higher H_2S levels under low-oxygen conditions may lead to greater U enrichment.

The PLI integrates contamination from multiple metals and presents a holistic assessment of sediment quality. This helps with spatial comparisons among stations and with identifying pollution hotspots. The PLI was calculated for all elements except Ti across sampling stations, and the results are presented in Figure 5a. A PLI value ≤ 1 indicates no metal pollution, while values greater than 1 indicate significant pollution [15]. The PLI values were >1 for stations MPA-1, MPA-3, and MPA-4, clearly indicating cumulative metal pollution, even when individual metals did not exceed the guideline thresholds. This shows that even when individual metals are present at low to moderate levels, their combined effects may still cause ecological stress, highlighting the need for multi-element indices [78]. Site-specific metal accumulation is indicated, as stations MPA-2 and MPA-5 had PLI values < 1, suggesting relatively unpolluted conditions.

The ecological risk index (RI), which incorporates metal toxicity and sums ecological risk factor (Er) values for trace metals, provides an integrated measure of ecological risk at each station (Figure 5b,c). RI values exceeded 150 at stations MPA-1 to MPA-4 within Sulaibikhat Bay, indicating a moderate ecological risk, while MPA-5 remained at low risk (Figure 5b). Cd had a high ecological risk factor (Er) at all stations, indicating its role in elevating the overall ecological risk (Figure 5c). This finding aligns with various coastal studies reporting Cd as the principal risk-driving metal due to its highly toxic response factor, even at moderate concentrations [79,80]. Agricultural inputs such as fertilisers and pesticides are a potential source of Cd contamination [79]. Hence, continuous monitoring and targeted mitigation strategies are needed to reduce Cd inputs to the MPA and address the significant environmental health concerns. In contrast, Cr, Ni, Cu, Zn, and Pb posed a low ecological risk, as their RI values were within low-risk categories, except at a few stations.

3.2.3. Toxicological Risk Indices

Sediment Quality Guidelines (SQGs) are reference values used to assess the harmful effects of sediment-associated contaminants on living organisms [81]. By comparing measured metal concentrations with established thresholds, such as ERL, ERM, TEL, and PEL (Table 1), it is possible to assess both individual and combined toxicological risks in benthic environments [82,83]. The ERL defines a concentration below which harmful effects on organisms are rarely observed. The ratio of measured metal concentrations to their respective ERL values is shown in Figure 6. Ratios < 1 indicate a low likelihood of ecological effects, whereas ratios > 1 suggest the potential for adverse biological impacts. Among the toxic metals analysed, the metal/ERL ratios for Cr, Ni, and Cu at MPA-1 to MPA-4 exceeded 1, suggesting potential ecological impacts. In contrast, all toxic metals at MPA-5 showed ratios below 1, indicating no toxicological concerns at this station located

outside Sulaibikhat Bay (Figure 6). Exceedance of the ERL typically indicates early warning conditions, in which ecological effects are possible but not yet widespread [83]. Such patterns are commonly reported in coastal sediments influenced by industrial discharges, urban runoff, and petroleum-related activities, where these metals are often associated with fine-grained sediments and organic matter [23,67,84,85]. In contrast, the consistently low metal-to-ERL ratios at MPA-5 indicate a negligible likelihood of biological impairment.

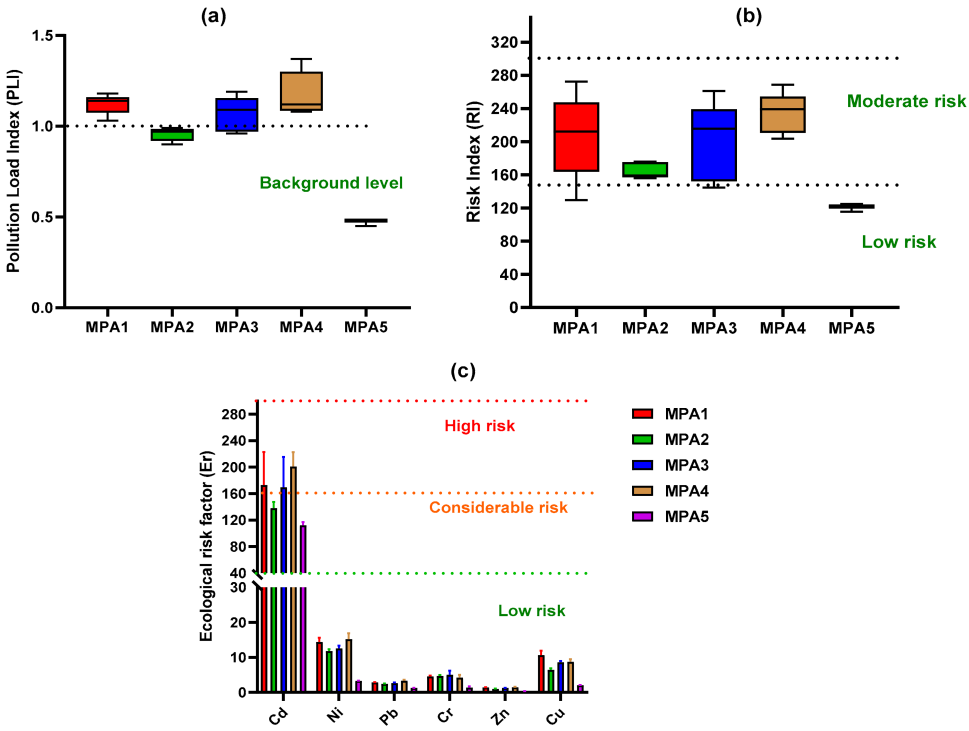


Figure 5. The pollution load index (**a**), ecological risk index (RI) (**b**) and ecological risk factor (**c**) of different stations in and around the marine protected area. Note: The ecological risk factor (Er), i.e., Risk level based on single metal: <40 → Low ecological risk; 40–80 → Moderate risk; 80–160 → Considerable risk; 160–320 → High risk; and >320 → Very high risk. The ecological risk index (RI), i.e., Risk level based on total ERI (all metals combined): <150 → Low risk; 150–300 → Moderate risk; 300–600 → Considerable risk; >600 → Very high ecological risk.

The ERM is the concentration above which harmful biological effects are likely to occur. The metal/ERM ratios are presented in Figure 7. A ratio < 1 suggests that toxic effects are unlikely, values around 1 indicate the onset of possible effects, and ratios > 1 imply a high probability of adverse biological effects. Elevated ERM ratios (>1) for Cu and Ni at MPA-1 to MPA-4 indicate that these stations may be at risk of toxicity from these metals.

However, MPA-5 was within a safe limit with less than 1 for all metals (Figure 7). Concentrations above ERM values are correlated with measurable toxicity in benthic organisms, including reduced survival, growth inhibition, and disturbance of community structure [85,86]. The low ERM value at MPA-5 reinforces the conclusion that this station is not subject to metal-induced ecological stress. Based on ERL and ERM analyses, although many stations showed early signs of contamination, only Cu and Ni reached concentrations associated with more serious and frequent toxicological effects.

Sediments are typically contaminated by complex mixtures of metals rather than individual elements; therefore, integrated indices, such as the mean PEL quotient (m-PEL-Q) and the mean ERM quotient (m-ERM-Q), are often used for assessing comprehensive toxicological risk [15,87]. The m-PEL-Q classifies sediments into four contamination categories: ≤0.1 (low contamination, ~8% probability of toxicity), 0.11–1.5 (low-moderate, ~21%),

1.5–2.30 (moderate to high, ~49%), ≥2.30 (high contamination, ~73% probability of toxicity) (Figure 8a,b). The m-PEL-Q values for the six toxic metals at all stations, except MPA 5, ranged from 0.1 to 1.5, suggesting low to moderate contamination and an approximate 21% probability of adverse toxic effects (Figure 8a) [88]. Although this probability does not indicate severe contamination, it suggests that benthic organisms may experience sublethal stress or episodic toxicity, particularly under unfavourable environmental conditions, such as low oxygen or sediment resuspension events. There is no significant toxicity in station MPA-5 as indicated by m-PEL-Q values (Figure 8a).

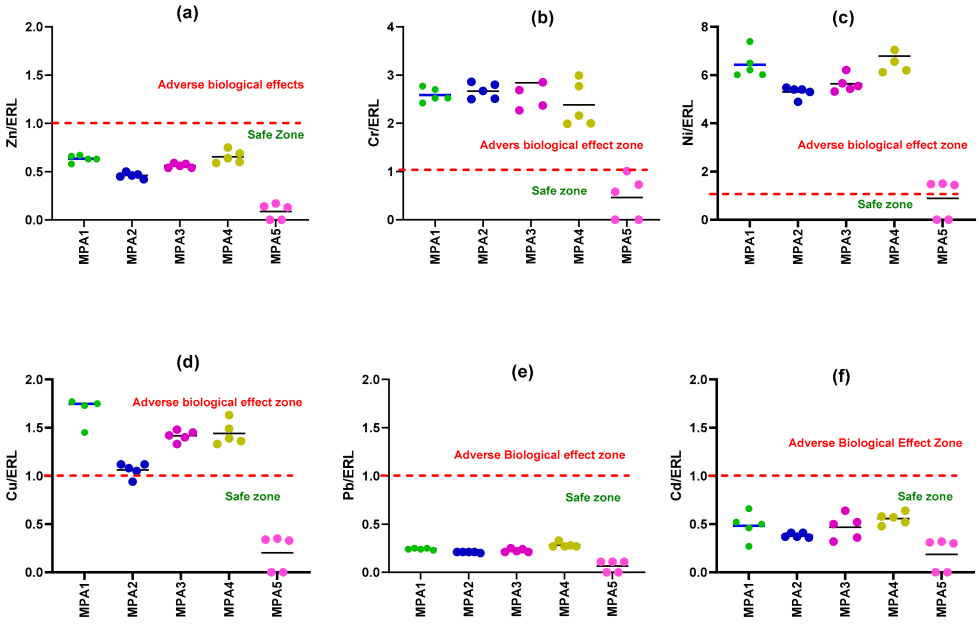


Figure 6. Ratios between the selected elements and the ERL levels in Sulaibikhat Bay MPA. Panels: (**a**) Zn, (**b**) Cr, (**c**) Ni, (**d**) Cu, (**e**) Pb and (**f**) Cd. If the ratio > 1, it is polluted, and if the ratio < 1, it is unpolluted. The red-dashed line separates the lower, non-polluted zone from the upper, polluted zone.

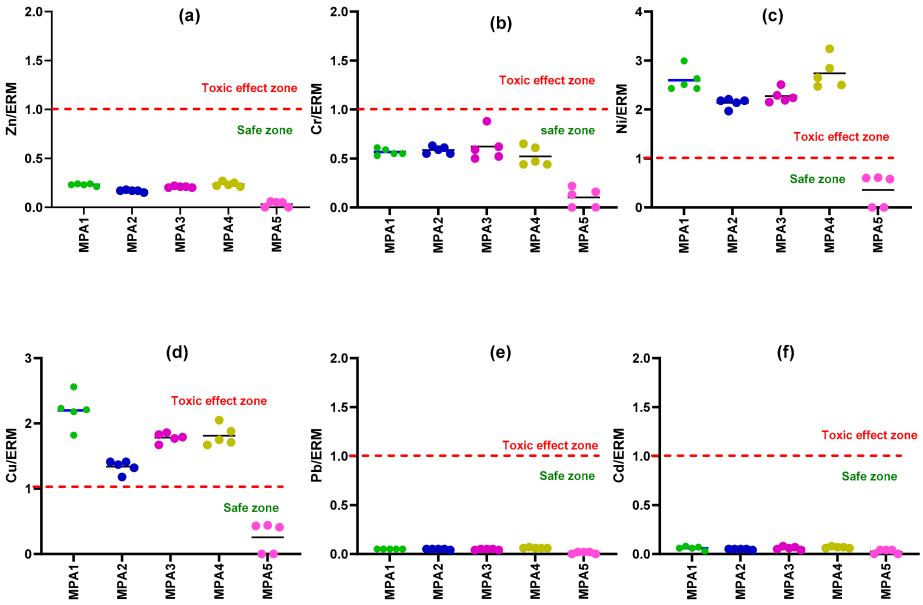


Figure 7. Ratios between the selected elements and the ERM levels in Sulaibikhat Bay MPA. Panels: (**a**) Zn, (**b**) Cr, (**c**) Ni, (**d**) Cu, (**e**) Pb and (**f**) Cd. If the ratio > 1 it is polluted and <1 it is unpolluted. The red dashed line separates the lower non-polluted zone from the upper polluted zone.

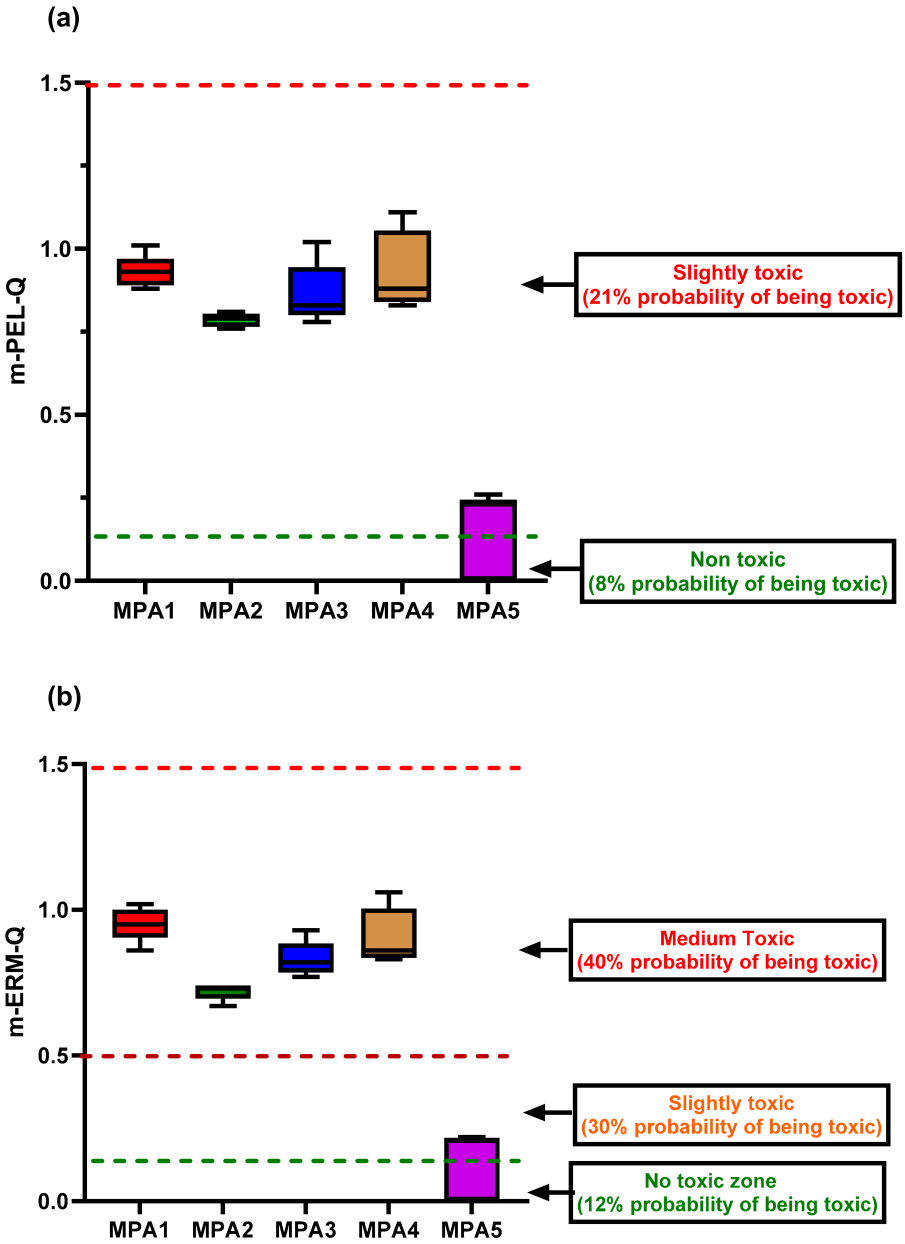


Figure 8. Spatial variation of toxicological risk indices for six trace metals (Cd, Cu, Cr, Pb, Ni, and Zn) in the surface sediments of the study region. (**a**) Mean PEL quotient (m-PEL-Q) and (**b**) Mean ERM quotient (m-ERM-Q).

The m-ERM-Q values provide a more stringent and more reliable estimate of toxicity and also highlight spatial differences among stations. In MPA-1 to MPA-4, the m-ERM-Q values indicated a moderate toxicity with an estimated 40% likelihood of biological effects. This was consistent with reported impacts in moderately contaminated coastal sediments worldwide [87,89]. These findings are consistent with higher ERM values for Cu and Ni, reinforcing their role as primary contributors to sediment toxicity in the Sulaibikhat Bay system. The station located outside Sulaibikhat bay showed lower m-ERM-Q values (Figure 8b), suggesting that this station represents a comparatively uncontaminated reference site within the study area.

4. Conclusions

This comprehensive study demonstrates that, despite the protected status, the Sulaibikhat MPA is still influenced by anthropogenic inputs from industrial, urban and

desalination activities. The dissolved metal concentrations were generally within acceptable limits, except for Cu. Sedimentary enrichment of Cd, Cr, and Ni indicates the localised contamination and the associated ecological risks. The spatial variability in contamination in comparison to a relatively unaffected reference site, together with PCA results, suggests that both local anthropogenic inputs and natural environmental factors contribute to metal distribution in Sulaibikhat Bay MPA. Overall, the findings indicate that formal MPA designation alone is not sufficient to mitigate trace metal contamination in this marine ecosystem. Continuous monitoring, effective source control, and adaptive management strategies are essential to safeguard the ecological integrity of the Sulaibikhat Bay MPA.

As the ecological implications presented in this study are inferred from sediment quality guidelines and contamination indices rather than direct biological observations, further investigations involving bioaccumulation in marine organisms, benthic community assessments, and ecotoxicological studies are required to validate the ecological significance of the observed metal enrichment.

Supplementary Materials: The following supporting information can be downloaded at: https://www.mdpi.com/article/10.3390/environments13070413/s1, Table S1: Certified reference material analysis for quality control of trace metal measurements for seawater; Table S2: Certified reference material analysis for quality control of trace metal measurements for sediment (mg/kg); Figure S1a. Spatio-temporal variations of Sr, Mo, Cd, Ba, Pb and Th at the surface sediment collected from Sulaibikhat Bay-MPA stations over four seasons (a to x); Figure S1b. Spatio-temporal variations of U, Al, Ti, V, Cr and Mn at the surface sediment collected from Sulaibikhat Bay-MPA stations over four seasons (a to x); Figure S1c. Spatio-temporal variations of Fe, Co, Ni, Cu and Zn at the surface sediment collected from Sulaibikhat Bay-MPA stations over four seasons (a-t).

Author Contributions: Conceptualization, T.A.-S. and F.A.-Y.; methodology, A.A.-H., L.F. and A.S.; formal analysis, A.A.-H., L.F., and A.S.; resources, W.A.-Z.; data curation, S.A., S.F.K.H., A.A.-H. and A.S.; writing—original draft preparation, S.A., S.F.K.H. and Y.P.; writing—review and editing, T.A.-S., S.A., S.F.K.H., A.A.-H., Y.P., R.M. and F.A.-Y.; supervision, T.A.-S. and F.A.-Y.; project administration, T.A.-S.; funding acquisition, T.A.-S. and F.A.-Y. All authors have read and agreed to the published version of the manuscript.

Funding: This research project SP002EC was funded by United Nations Compensation Commission (UNCC) through the Kuwait National Focal Point, project claim 5000460 and The APC was funded by the project SP002EC.

Data Availability Statement: The raw data supporting the conclusions of this article will be made available by the authors on request.

Acknowledgments: The authors gratefully acknowledge Takahiro Yamomoto for his assistance in the preparation map marked with the pollution source. We also thank Ayaz Ahmed, Gopikrishna Mantha, Nityanandan Manickam, Shajim Sainulubdeen, Sasi Kumar, and Babul Jalaladas for their valuable contributions to sample collection. The support and commitment of all project personnel are sincerely appreciated.

Conflicts of Interest: The authors declare no conflicts of interest.

References

1. Halpern, B.S.; Frazier, M.; Potapenko, J.; Casey, K.S.; Koenig, K.; Longo, C.; Lowndes, J.S.; Rockwood, R.C.; Selig, E.R.; Selkoe, K.A.; et al. Spatial and temporal changes in cumulative human impacts on the world's ocean. *Nat. Commun.* **2015**, *6*, 8615. [CrossRef] [PubMed]
2. Ban, N.C.; Davies, T.E.; Aguilera, S.E.; Brooks, C.; Cox, M.; Epstein, G.; Evans, L.S.; Maxwell, S.M.; Nenadovic, M. Social and ecological effectiveness of large marine protected areas. *Glob. Environ. Chang.* **2017**, *43*, 82–91. [CrossRef]

3. Giakoumi, S.; McGowan, J.; Mills, M.; Beger, M.; Bustamante, R.H.; Charles, A.; Christie, P.; Fox, M.; Garcia-Borboroglu, P.; Gelcich, S.; et al. Revisiting "Success" and "Failure" of marine protected areas: A conservation scientist perspective. *Front. Mar. Sci.* **2018**, *5*, 223. [CrossRef]
4. Hasan, M.; Rahman, M.; al Ahmed, A.; Islam, M.A.; Rahman, M. Heavy metal pollution and ecological risk assessment in the surface water from a marine protected area, Swatch of No Ground, north-western part of the Bay of Bengal. *Reg. Stud. Mar. Sci.* **2022**, *52*, 102278. [CrossRef]
5. Ghaemi, M.; Soleimani, F.; Gholamipour, S. Heavy metal and persistent organic pollutant profile of sediments from marine protected areas: The northern Persian Gulf. *Environ. Sci. Pollut. Res.* **2023**, *30*, 120877–120891. [CrossRef] [PubMed]
6. Ba, I.; Diankha, O.; Ali Sow, B.; Ba, S. Assessment of sediment quality in the Sangomar marine protected area in Senegal prior to oil development. *Open J. Mar. Sci.* **2025**, *15*, 157–172. [CrossRef]
7. Abessa, D.M.; Albuquerque, H.C.; Morais, L.G.; Araújo, G.S.; Fonseca, T.G.; Cruz, A.C.; Campos, B.G.; Camargo, J.B.; Gusso-Choueri, P.K.; Perina, F.C.; et al. Pollution status of marine protected areas worldwide and the consequent toxic effects are unknown. *Environ. Pollut.* **2018**, *243*, 1450–1459. [CrossRef] [PubMed]
8. Moreira, L.B.; Fernandes, G.M.; Figueira, R.C.L.; do Nascimento, R.F.; Cavalcante, R.M.; Machado, W.T.V.; Abessa, D.M.D.S. Sediment contamination and toxicity of Marine Protected Areas in southeastern Brazilian coast: A baseline for management planning. *Mar. Pollut. Bull.* **2021**, *170*, 112613. [CrossRef] [PubMed]
9. Ghaemi, M.; Soleimani, F.; Arfaeinia, H.; Gholamipour, S. Distribution, environmental risks, and conservation challenges of chemical pollutants in Persian Gulf marine protected areas. *Sci. Rep.* **2024**, *14*, 26343. [CrossRef] [PubMed]
10. Lubis, A.A.; Sugiharto, U.; Putra, A.D.P.; Shintianata, D. Historical trend of heavy metals in mangrove sediment from Nusa Lembongan, Bali using 210Pb-geochronology. *IOP Conf. Ser. Earth Environ. Sci.* **2023**, *1251*, 012020. [CrossRef]
11. Sim, V.X.; Dafforn, K.A.; Simpson, S.L.; Kelaher, B.P.; Johnston, E.L. Sediment contaminants and infauna associated with recreational boating structures in a multiuse marine park. *PLoS ONE* **2015**, *10*, e0130537. [CrossRef] [PubMed]
12. Zhang, Y.; Chu, C.; Li, T.; Xu, S.; Liu, L.; Ju, M. A water quality management strategy for regionally protected water through health risk assessment and spatial distribution of heavy metal pollution in 3 marine reserves. *Sci. Total Environ.* **2017**, *599*, 721–731. [CrossRef] [PubMed]
13. Semprucci, F.; Appolloni, L.; Grassi, E.; Donnarumma, L.; Cesaroni, L.; Tirimberio, G.; Chianese, E.; Di Donato, P.; Russo, G.F.; Balsamo, M.; et al. Antarctic special protected area 161 as a reference to assess the effects of anthropogenic and natural impacts on meiobenthic assemblages. *Diversity* **2021**, *13*, 626. [CrossRef]
14. Amin, S.A.; Almahasheer, H. Pollution indices of heavy metals in the Western Arabian Gulf coastal area. *Egypt. J. Aquat. Res.* **2022**, *48*, 21–27. [CrossRef]
15. Elobaid, E.A.; Yigiterhan, O.; Al-Ansari, E.M.S.; Chen, Z.; Mohieldeen, Y.; Abdalla, R. Ecological risk assessment of heavy metals in the marine sediments associated with the petroleum hydrocarbon industry in the central Arabian Gulf. *J. Hazard. Mater. Adv.* **2025**, *19*, 100749. [CrossRef]
16. Shalini, R.; Jeyasekaran, G.; Shakila, R.J.; Sundhar, S.; Arisekar, U.; Jawahar, P.; Aanand, S.; Sivaraman, B.; Malini, A.H.; Surya, T. Dietary intake of trace elements from commercially important fish and shellfish of Thoothukudi along the southeast coast of India and implications for human health risk assessment. *Mar. Pollut. Bull.* **2021**, *173*, 113020. [CrossRef] [PubMed]
17. Santhosh, K.; Kamala, K.; Ramasamy, P.; Musthafa, M.S.; Almujri, S.S.; Basheeruddin, S.M.; Sivaperumal, P. Unveiling the silent threat: Heavy metal toxicity, devastating impact on aquatic organisms, and DNA damage. *Mar. Pollut. Bull.* **2024**, *200*, 116139. [CrossRef] [PubMed]
18. Yu, C.; Du, W.; Meng, K.; Chen, X.; Zhang, H.; Xu, M. Exploring the potential ecological risks of cadmium accumulation in coastal sediments: Implications for diversity, function, and assembly of fungal community. *J. Environ. Manag.* **2025**, *395*, 127726. [CrossRef]
19. Johansen, J.L.; Mitchell, M.D.; Vaughan, G.O.; Ripley, D.M.; Shiels, H.A.; Burt, J.A. Impacts of ocean warming on fish size reductions on the World's hottest coral reefs. *Nat. Commun.* **2024**, *15*, 5457. [CrossRef] [PubMed]
20. Hosseini, H.; Saadaoui, I.; Moheimani, N.; Al Saidi, M.; Al Jamali, F.; Al Jabri, H.; Hamadou, R.B. Marine health of the Arabian Gulf: Drivers of pollution and assessment approaches focusing on desalination activities. *Mar. Pollut. Bull.* **2021**, *164*, 112085. [CrossRef] [PubMed]
21. Al-Said, T.; Madhusoodhanan, R.; Pokavanich, T.; Al-Yamani, F.; Kedila, R.; Al-Ghunaim, A.; Al-Hashem, A. Environmental characterization of a semiarid hyper saline system based on dissolved trace metal-macronutrient synergy: A multivariate spatio-temporal approach. *Mar. Pollut. Bull.* **2018**, *129*, 846–858. [CrossRef] [PubMed]
22. El-Anbaawy, M.; Abdelhalim, A.; Al Ajmi, D.; Al Sarawi, M. Environmental assessment and evaluation of anthropogenic impacts on Sulaibikhat Bay tidal flat area, Kuwait. *J. Health Environ. Res.* **2018**, *4*, 21–34. [CrossRef]
23. Lyons, B.P.; Devlin, M.J.; Hamid, S.A.; Al-Otiabi, A.F.; Al-Enezi, M.; Massoud, M.S.; Al Zaidan, A.S.; Smith, A.J.; Morris, S.; Bersuder, P.; et al. Microbial water quality and sedimentary faecal sterols as markers of sewage contamination in Kuwait. *Mar. Pollut. Bull.* **2015**, *100*, 689–698. [CrossRef] [PubMed]

24. Al Mukaimi, M.E.; Cerv, J.; Dellapenna, T.; Alaskar, H.; Dashti, J.; Esmaeil, A. Spatial analysis of total mercury concentration in surface sediments in Sulaibikhat Bay, Kuwait. *Mar. Pollut. Bull.* **2025**, *214*, 117793. [CrossRef] [PubMed]
25. Habeebullah, S.F.K.; Al Said, T.; Alagarsamy, S.; Ahamed, N.; Martinez, K.; Abusam, A.; Madhusoodhanan, R.; Al Shamali, M.; Al-Zekri, W.; Al Yamani, F. Pollution dynamics in the first marine protected area of the Northwestern Arabian Gulf: Environmental assessment and management implications. *Environ. Pollut.* **2025**, *369*, 125856. [CrossRef]
26. Alshemmari, H.; Al-Dousari, A.M.; Talebi, L.; Al-Ghadban, A.N. Mineralogical characteristics of surface sediment in Sulaibikhat Bay, Kuwait. *Kuwait J. Sci.* **2013**, *40*, 159–176.
27. Al-Said, T.; Al-Kandari, M.; Madhusoodhanan, R.; Al-Yamani, F.; Sarkar, A.; Yamamoto, T.; Farvin, S.; Al-Ghunaim, A.; Al-Zekri, W.; Ahmad, A.; et al. *Marine Protected Area in Sulaibikhat Bay—Project Claim 5000460. Physicochemical Assessment and Biological Oceanography of the Marine Protected Area;* Final Rep. I & II; Kuwait Institute for Scientific Research: Kuwait City, Kuwait, 2022; 783p.
28. Schlitzer, R.; Anderson, R.F.; Dodas, E.M.; Lohan, M.; Geibert, W.; Tagliabue, A.; Bowie, A.; Jeandel, C.; Maldonado, M.T.; Landing, W.M.; et al. The GEOTRACES intermediate data product 2017. *Chem. Geol.* **2018**, *493*, 210–223. [CrossRef]
29. Hu, Z.; Qi, L. Sample digestion methods. In *Treatise on Geochemistry*; Turekian, K.K., Ed.; Elsevier: Amsterdam, The Netherlands, 2014; Volume 1, pp. 87–109.
30. Abdullah, M.I.C.; Sah, A.S.R.M.; Haris, H. Geoaccumulation index and enrichment factor of arsenic in surface sediment of Bukit Merah Reservoir, Malaysia. *Trop. Life Sci. Res.* **2020**, *31*, 109. [CrossRef] [PubMed]
31. Rudnick, R.L.; Gao, S. Composition of the continental crust. In *Treatise on Geochemistry*, 2nd ed.; Holland, H.D., Turekian, K.K., Eds.; Elsevier: Amsterdam, The Netherlands, 2014; Volume 4, pp. 1–51. [CrossRef]
32. Benson, N.U.; Anake, W.U.; Essien, J.P.; Enyong, P.; Olajire, A.A. Distribution and risk assessment of trace metals in Leptodius exarata, surface water, and sediments from Douglas Creek in the Qua Iboe Estuary. *J. Taibah Univ. Sci.* **2017**, *11*, 434–449. [CrossRef]
33. Hackson, L. An ecological risk index for aquatic pollution control. A sedimentological approach. *Water Res.* **1980**, *14*, 975–1001. [CrossRef]
34. Long, E.R.; Morgan, L.G. The potential for biological effects of sediment sorbed contaminants tested in the National Status and Trends Program. In *NOAA Technical Memorandum NOS OMA 52*; National Oceanic and Atmospheric Administration: Seattle, WA, USA, 1990.
35. Buchman, M.F. *Screening Quick Reference Tables—Squirts*; NOAA: Silver Spring, MD, USA, 2008. Available online: https://repository.library.noaa.gov/view/noaa/9327 (accessed on 15 May 2026).
36. Zheng, L.; Minami, T.; Takano, S.; Sohrin, Y. Distributions of cadmium, nickel, zinc, copper, and iron in the western South Pacific Ocean: Local sources of the nutrient-type trace metals. *Mar. Chem.* **2024**, *263*, 104411. [CrossRef]
37. Sabarathinam, C.; Bhandary, H.; Al-Khalid, A. A geochemical analogy between the metal sources in Kuwait Bay and territorial sea water of Kuwait. *Environ. Monit. Assess.* **2019**, *191*, 142. [CrossRef] [PubMed]
38. Ahmady-Birgani, H.; McQueen, K.G.; Mirnejad, H. Characteristics of mineral dust impacting the Persian Gulf. *Aeolian Res.* **2018**, *30*, 11–19. [CrossRef]
39. Bu-Olayan, A.H.; Subrahmanyam, M.N.V.; Al-Sarawi, M.; Thomas, B.V. Effects of the Gulf War oil spill in relation to trace metals in water, particulate matter and PAHs from the Kuwaiti coast. *Environ. Int.* **1998**, *24*, 789–797.
40. Bu-Olayan, A.H.; Al-Hassan, R.; Thomas, B.V.; Subrahmanyam, M.N.V. Impact of trace metals and nutrients levels on phyto-plankton from the Kuwait Coast. *Environ. Int.* **2001**, *26*, 199–203. [CrossRef] [PubMed]
41. Al-Sarawi, M.A.; Massoud, M.S.; Khader, S.R.; Bou-Olyan, A.H. Recent trace metal levels in coastal waters of Sulaibikhat Bay, Kuwait. *Technology* **2002**, *8*, 27–38.
42. Al-Said, T.F.; Pokavanich, T.; Al-Hashem, A.; Kedila, R. Distribution of Bioactive Trace Metals (Fe, Co, Ni, Cu and Zn) in the semiarid Kuwait Bay, stressed by natural and anthropogenic processes. In *American Geophysical Union, Ocean Sciences Meeting*; American Geophysical Union (AGU): New Orleans, LA, USA, 2016; p. CT34B-0192.
43. Al-Qattan, F.; Al-Sarawi, M. Water quality assessment and bottom sediment in the coastal area of the three refineries (Mina Al-Ahmadi, Mina Shuaiba and Mina Abdullah), Kuwait. *J. Environ. Pollut. Hum. Health* **2017**, *5*, 69–82.
44. Nour, H.E.; Ramadan, F.; Alsubaie, K.; Tawfik, M. Seasonal variation and assessment of heavy metals in coastal seawater of Kuwait Bay, northeast coast of Kuwait. *Environ. Asia* **2022**, *15*, 108–119.
45. Seoud, M.S.; Abbas, Y.M.; Helal, A.E.F.I.; Salama, S.; Mansour, N.A. Evaluation of heavy, toxic and trace metals contamination in fish, seawater, sediments and seashells of the Arabian Gulf coastal, Kuwait. *Ecosystems* **2021**, *2*, 3.
46. Dippong, T.; Resz, M.A. Heavy metal contamination assessment and potential human health risk of water quality of lakes situated in the protected area of Tisa, Romania. *Heliyon* **2024**, *10*, e28860. [CrossRef] [PubMed]
47. Nicolaus, E.E.M.; Wright, S.R.; Barry, J.; Bolam, T.P.C.; Ghareeb, K.; Ghaloom, M.; Al-Kanderi, N.; Harley, B.F.M.; Le Quesne, W.J.F.; Devlin, M.J.; et al. Spatial and temporal analysis of the risks posed by total petroleum hydrocarbon and trace element contaminants in coastal waters of Kuwait. *Mar. Pollut. Bull.* **2017**, *120*, 422–427. [CrossRef] [PubMed]

48. Maher, B.; Prospero, J.M.; Mackie, D.; Gaiero, D.; Hesse, P.P.; Balkanski, Y. Global connections between aeolian dust, climate and ocean biogeochemistry at the present day and at the last glacial maximum. *Earth Sci. Rev.* **2010**, *99*, 61–97. [CrossRef]
49. Ezzati, R. An investigation on atmospheric dust which transport to the Persian Gulf. *J. Oceanogr.* **2012**, *2*, 21–30.
50. Abdel Satar, A.M.; Abdel Fattah, N.M.; Mohamed, A. Water–sediment interactions and mobility of heavy metals in aquatic environments. *Water Res.* **2021**, *202*, 117386. [CrossRef] [PubMed]
51. Al-Jber, R.; Al-Sarawi, M. Assessment of heavy metals and total petroleum hydrocarbons in bottom sediments of Kuwait Bay. *Am. J. Environ. Prot.* **2024**, *13*, 234–245. [CrossRef]
52. Boota, A.A.; Al-Enezi, E. Assessing sediment contamination in Kuwait Bay: A comprehensive environmental analysis of effluent discharge impact. *Int. J. Sustain. Dev. Plan.* **2023**, *18*, 3449–3458. [CrossRef]
53. Alshemmari, H.; Talebi, L. Heavy metal concentrations in the surface sediments of the northwestern Arabian Gulf, Kuwait. *Arab. J. Geosci.* **2019**, *12*, 565. [CrossRef]
54. Alshemmari, H.; Alotaibi, Y.; Owens, R. Trace metal concentrations in the surface sediments of Sulaibikhat Bay, Kuwait. *Kuwait J. Sci. Eng.* **2010**, *37*, 87–100.
55. Alshraifi, F.; Alkandari, A.; Al-Khalaf, B.; Al-Rifay, I.; Al-Mudhf, H.F. Trace metals and total organic carbon concentrations at intertidal area in Sulaibikhat Bay. *Kuwait J. Sci. Eng.* **2009**, *36*, 125–145.
56. Hassan, I.S.; Bahman, H.H. Geoindicator of heavy metals contamination in bottom sediments of Kuwait Bay, northwestern Arabian Gulf. *Egypt. J. Geol.* **2025**, *69*, 283–298. [CrossRef]
57. Sojka, M.; Jaskuła, J.; Barabach, J.; Ptak, M.; Zhu, S. Heavy metals in lake surface sediments in protected areas in Poland: Concentration, pollution, ecological risk, sources and spatial distribution. *Sci. Rep.* **2022**, *12*, 15006. [CrossRef] [PubMed]
58. Asteman, I.P.; Van Nieuwenhove, N.; Andersen, T.J.; Linders, T.; Nordberg, K. Recent environmental change in the Kosterhavet National Park marine protected area as reflected by hydrography and sediment proxy data. *Mar. Environ. Res.* **2021**, *166*, 105265. [CrossRef]
59. Araujo, G.S.; Gusso-Choueri, P.K.; Favaro, D.I.T.; Rocha, R.C.C.; Saint'Pierre, T.D.; Hauser-Davis, R.A.; Braz, B.; Santelli, R.E.; Freire, A.S.; Machado, W.T.V.; et al. Metal-associated biomarker responses in crabs from a marine protected area in southeastern Brazil. *Arch. Environ. Contam. Toxicol.* **2020**, *78*, 463–477. [CrossRef] [PubMed]
60. Perina, F.C.; Abessa, D.M.D.S. Contamination and toxicity in a subtropical estuarine protected area influenced by former mining activities. *Ocean Coast. Res.* **2020**, *68*, e20313. [CrossRef]
61. Fuentes-Gandara, F.; Pinedo-Hernández, J.; Gutiérrez, E.; Marrugo-Negrete, J.; Díez, S. Heavy metal pollution and toxicity assessment in Mallorquin swamp: A natural protected heritage in the Caribbean Sea, Colombia. *Mar. Pollut. Bull.* **2021**, *167*, 112271. [CrossRef] [PubMed]
62. Jasser, S.; Al-Sarawi, M.; Khader, S. Recent trace metals pollution in bottom sediments of Khor Al-Sabiya, Kuwait. *J. Coast Zone Manag.* **2017**, *20*, 2–18. [CrossRef]
63. Hanson, P.J.; Evans, D.W.; Colby, D.R.; Zdanowicz, V.S. Assessment of elemental contamination in estuarine and coastal environments based on geochemical and statistical modeling of sediments. *Mar. Environ. Res.* **1993**, *36*, 237–266. [CrossRef]
64. Napoletano, P.; Napoletano, P.; Colombo, C.; Memoli, V.; Speranza, C.; Ruggiero, A.; Santorufo, L.; Maisto, G.; De Marco, A.; De Marco, A. Integrated approach for quality assessment of technosols in experimental mesocosms. *Sustainability* **2021**, *13*, 9101. [CrossRef]
65. Bueno, C.; Figueira, R.; Ivanoff, M.D.; Junior, E.E.T.; Fornaro, L.; García-Rodríguez, F. A multi proxy assessment of long-term anthropogenic impacts in Patos Lagoon, southern Brazil. *J. Sediment. Environ.* **2019**, *4*, 276–290. [CrossRef]
66. Zhang, J.; Liu, C.L. Riverine composition and estuarine geochemistry of particulate metals in China weathering features, anthropogenic impact, and chemical fluxes. *Estuar. Coast. Shelf Sci.* **2002**, *54*, 1051–1070. [CrossRef]
67. Nicolaus, E.E.M.; Maxwell, D.L.; Khamis, A.S.; Abdulla, K.H.; Harrod, R.P.; Devlin, M.J.; Lyons, B.P. Spatial and temporal analysis of the risks posed by metal contamination in coastal and marine sediments of Bahrain. *Environ. Monit. Assess.* **2022**, *194*, 62. [CrossRef] [PubMed]
68. Al-Abdali, F.; Massoud, M.S.; Al-Ghadban, A.N. Bottom sediments of the Arabian Gulf-III. Trace metal contents as indicators of pollution and implications for the effect and fate of the Kuwait oil slick. *Environ. Pollut.* **1996**, *93*, 285–301. [CrossRef] [PubMed]
69. Templeton, D.M.; Liu, Y. Multiple roles of cadmium in cell death and survival. *Chem.-Biol. Interact.* **2010**, *188*, 267–275. [CrossRef] [PubMed]
70. El-Sharkawy, M.; Alotaibi, M.O.; Li, J.; Du, D.; Mahmoud, E. Heavy metal pollution in coastal environments: Ecological implications and management strategies: A review. *Sustainability* **2025**, *17*, 701. [CrossRef]
71. Turekian, K.K. The marine geochemistry of strontium. *Geochim. Cosmochim. Acta* **1964**, *28*, 1479–1496. [CrossRef]
72. Algeo, T.J.; Tribovillard, N. Environmental analysis of paleoceanographic systems based on molybdenum–uranium covariation. *Chem. Geol.* **2009**, *268*, 211–225. [CrossRef]
73. Tribovillard, N.; Algeo, T.J.; Baudin, F.; Riboulleau, A. Analysis of marine environmental conditions based on molybdenum–uranium covariation—Applications to Mesozoic paleoceanography. *Chem. Geol.* **2012**, *324*, 46–58. [CrossRef]

74. Helz, G.R.; Miller, C.V.; Charnock, J.M.; Mosselmans, J.F.W.; Pattrick, R.A.D.; Garner, C.D.; Vaughan, D.J. Mechanism of molybdenum removal from the sea and its concentration in black shales: EXAFS evidence. *Geochim. Cosmochim. Acta* **1996**, *60*, 3631–3642. [CrossRef]
75. Zheng, Y.; Anderson, R.F.; Van Geen, A.; Fleisher, M.Q. Remobilization of authigenic uranium in marine sediments by bioturbation. *Geochim. Cosmochim. Acta* **2002**, *66*, 1759–1772. [CrossRef]
76. Zheng, Y.; Anderson, R.F.; Van Geen, A.; Fleisher, M.Q. Preservation of particulate non-lithogenic uranium in marine sediments. *Geochim. Cosmochim. Acta* **2002**, *66*, 3085–3092. [CrossRef]
77. Crusius, J.; Calvert, S.; Pedersen, T.; Sage, D. Rhenium and molybdenum enrichments in sediments as indicators of oxic, suboxic and sulfidic conditions of deposition. *Earth Planet. Sci. Lett.* **1996**, *145*, 65–78. [CrossRef]
78. Tomlinson, D.L.; Wilson, J.G.; Harris, C.R.; Jeffrey, D.W. Problems in the assessment of heavy-metal levels in estuaries and the formation of a pollution index. *Helgol. Meeresunters.* **1980**, *33*, 566–575. [CrossRef]
79. Mejjad, N.; El Aouidi, S.; Laissaoui, A. Assessment of potential ecological risks of Cr, Cd, Pb, and As in coastal sediments. *Proceedings* **2024**, *102*, 53. [CrossRef]
80. Yu, C.; Meng, K.; Zhu, Z.; Liu, S.; Zhou, Z.; Zhang, H.; Xu, M. Impacts of cadmium accumulation on the diversity, assembly processes, and co-occurrence patterns of archaeal communities in marine sediments. *Sci. Total Environ.* **2024**, *926*, 171936. [CrossRef] [PubMed]
81. Kara, H. Geochemical assessment of potentially toxic elements in urban stream sediments draining into the keban dam Lake, Turkey. *Appl. Sci.* **2025**, *15*, 7565. [CrossRef]
82. Long, E.R.; Field, L.J.; MacDonald, D.D. Predicting toxicity in marine sediments with numerical sediment quality guidelines. *Environ. Toxicol. Chem.* **1998**, *17*, 714–727. [CrossRef]
83. MacDonald, D.D.; Ingersoll, C.G.; Berger, T.A. Development and evaluation of consensus-based sediment quality guidelines for freshwater ecosystems. *Arch. Environ. Contam. Toxicol.* **2000**, *39*, 20–31. [CrossRef] [PubMed]
84. Birch, G.F. A review of chemical-based sediment quality assessment methodologies for the marine environment. *Mar. Pollut. Bull.* **2018**, *133*, 218–232. [CrossRef] [PubMed]
85. Abedi, E.; Nozarpour, R. Assessment of PAH and heavy metal contamination in the Pars Special Economic Energy Zone surface sediments: Ecological implications and source identification. *Environ. Sci. Pollut. Res.* **2025**, *32*, 23574–23587. [CrossRef]
86. Watson, G.J.; Pini, J.M.; Richir, J.; Michie, L.A. Detecting the effects of chronic metal exposure on benthic systems: Importance of biomarker and endpoint selection. *Aquat. Toxicol.* **2021**, *230*, 105674. [CrossRef] [PubMed]
87. Long, E.R.; MacDonald, D.D.; Severn, C.G.; Hong, C.B. Classifying probabilities of acute toxicity in marine sediments with empirically derived sediment quality guidelines. *Environ. Toxicol. Chem.* **2000**, *19*, 2598–2601. [CrossRef]
88. Yi, Y.J.; Sun, J.; Tang, C.H.; Zhang, S.H. Ecological risk assessment of heavy metals in sediment in the upper reach of the Yangtze River. *Environ. Sci. Pollut. Res.* **2016**, *23*, 11002–11013. [CrossRef]
89. Badr, N.B.; El-Fiky, A.A.; Mostafa, A.R.; Al-Mur, B.A. Metal pollution records in core sediments of some Red Sea coastal areas, Kingdom of Saudi Arabia. *Environ. Monit. Assess.* **2009**, *155*, 509–526. [PubMed]

Disclaimer/Publisher's Note: The statements, opinions and data contained in all publications are solely those of the individual author(s) and contributor(s) and not of MDPI and/or the editor(s). MDPI and/or the editor(s) disclaim responsibility for any injury to people or property resulting from any ideas, methods, instructions or products referred to in the content.